MODAL CHARACTERIZATION OF A PIEZOELECTRIC SHAKER TABLE

THESIS
MARCH 2015

Randall J. Hodkin Jr., Captain, USAF

AFIT-ENY-MS-15-J-001

DEPARTMENT OF THE AIR FORCE
AIR UNIVERSITY

AIR FORCE INSTITUTE OF TECHNOLOGY

Wright-Patterson Air Force Base, Ohio

AFIT-ENY-MS-15-J-001

MODAL CHARACTERIZATION OF A PIEZOELECTRIC SHAKER TABLE

THESIS

Presented to the Faculty

Department of Aeronautics and Astronautics

Graduate School of Engineering and Management

Air Force Institute of Technology

Air University

Air Education and Training Command

In Partial Fulfillment of the Requirements for the

Degree of Master of Science in Aeronautical Engineering

Randall J. Hodkin Jr., BS

Captain, USAF

June 2015

AFIT-ENY-MS-15-J-001

MODAL CHARACTERIZATION OF A PIEZOELECTRIC SHAKER TABLE

Randall J. Hodkin Jr., BS

Captain, USAF

Committee Membership:

Dr. A. N. Palazotto
Chair

Dr. M. B. Ruggles-Wrenn
Member

Lt Col A. M. DeLuca, PhD
Member

Dr. O. E. Scott-Emuakpor
Member

AFIT-ENY-MS-15-J-001

Abstract

Piezoelectric actuated shaker tables are often used for high frequency fatigue testing. Since natural frequencies can appear in the operating range of these shaker tables, it is necessary to conduct modal characterization of the system before testing. This thesis describes the design and experimental validation of a mechanical model used for modal analysis of a piezoelectric shaker table. A commercially available three-dimensional scanning device was used to produce a point cloud model of the surface geometry, which was converted to a solid model and imported into a Finite Element Analysis (FEA) package for modal analysis. Using a laser vibrometer to measure displacement and velocity, the physical vibration response of the shaker table was obtained for comparison with FEA frequency response results. The laser vibrometer data was used to validate and tune the FEA modal response.

Acknowledgments

I would like to thank my thesis advisor and mentor, Dr. Anthony Palazotto, for his direction, insight, and encouragement during the course of this thesis effort. I would also like to thank Dr. Tommy George and all of the helpful people in the Turbine Engine Fatigue Facility at the Air Force Research Labs for the knowledge and time provided to support me in completing this thesis.

Randall J. Hodkin Jr.

Table of Contents

Page

List of Figures

Page

List of Tables

Page

List of Symbols

A	Area or Piezoelectric Crystal Excitation Amplitude
AFRL	Air Force Research Laboratory
ATOS	Advanced Topometric Sensor
b	Beam Width
c	Constant Coefficient of Friction or Viscous Damping Coefficient
CAD	Computer Aided Design
CSV	Comma Separated Values
C_1	Differential Equation Solution Constant
C_2	Differential Equation Solution Constant
[C]	Finite Element Damping Matrix
[c]	Piezo Material Elasticity Constants Matrix
D	Piezoelectric Shaker Table Bolt Diameter
DEOM	Differential Equation of Motion
d_{ij}	Piezoelectric Deformation Coefficient
DOF	Degrees of Freedom
D_1	Differential Equation Solution Constant
D_2	Differential Equation Solution Constant
d_{33}	Piezoelectric Longitudinal Deformation Coefficient
{D}	Piezo Material Electric Displacement Matrix
δ	Displacement
E	Modulus of Elasticity
EOM	Equation of Motion
{E}	Piezo Material Electric Field Matrix
[e]	Piezoelectric Coupling Coefficients Matrix
{ε}	Piezo Material Dielectric Constants Matrix
F	Force
FBD	Free Body Diagram
f_d	Doppler Effect Frequency Shift
FEA	Finite Element Analysis
FEM	Finite Element Model
F_{pre}	Pre-Load Force Applied by Tightened Shaker Table Bolts
F(t)	Equation of Motion Forcing Function
{F}	Finite Element Force Matrix
ζ	Viscous Damping Factor
g	Acceleration due to Gravity
GOM	Gesellschaft für Optische Messtechnik
GPU	Graphics Processing Unit
G(ω)	Frequency Response Function
h	Beam Height
HPC	High Performance Computing
Hz	Hertz
I	Moment of Inertia
IE	Isolation Efficiency
IGES	Initial Graphics Exchange Specification
k	Stiffness

k_b	Simplified Model Beam Stiffness
k_{eq}	Equivalent Stiffness
KD	Kinetic Diagram
k_p	Simplified Model Piezoelectric Stack Stiffness
[K]	Finite Element Stiffness Matrix
L	Length
λ	Wavelength
M	Mass
MPC	Multi Point Constraint
[M]	Finite Element Mass Matrix
n	Number of Piezoelectric Crystal in a Stack
PZT	Lead (Pb), Zirconate (Z), Titanate (Ti) Piezoelectric Ceramic
s	Characteristic Equation Root
STL	Stereo Lithography
SDOF	Single Degree of Freedom
σ_y	Yield Strength
t	Time or Thickness
T	Piezoelectric Shaker Table Bolt Torque
TEFF	Turbine Engine Fatigue Facility
T_{iso}	Isolation Pad Transmissibility
{T}	Piezo Material Stress Matrix
{u}	Finite Element Displacement Matrix
$\{\dot{u}\}$	Finite Element Velocity Matrix
$\{\ddot{u}\}$	Finite Element Acceleration Matrix
v	Velocity
V	Voltage
ω	Driven Frequency
ω_n	Natural Frequency
x	Simplified Model Displacement from Non-Equilibrium Position
$\ddot{x}$	Simplified Model Acceleration about Non-Equilibrium Position
y	Simplified Model Displacement from Equilibrium Position
$\ddot{y}$	Simplified Model Acceleration about Equilibrium Position
y_h	Equation of Motion Homogeneous Solution
y_p	Equation of Motion Particular Solution
2D	Two-Dimensional
3D	Three-Dimensional

MODAL CHARACTERIZATION OF A PIEZOELECTRIC SHAKER TABLE

I. Introduction

Problem Statement

The Air Force Research Laboratory (AFRL) Turbine Engine Fatigue Facility (TEFF) conducts structural characterization studies pertaining to turbine engine components. The TEFF frequently uses vibration shakers to apply multiple load cycles to a specimen to conduct fatigue loading tests. Shaker tables used in these tests have an operational frequency range which limits how many load cycles can be applied in a given time. However, many advanced turbine engine components requiring one billion load cycles under the Turbine Engine Structural Integrity Program (ENSIP), are regularly tested in a single day. To meet these high cycle testing demands, it is often desirable for the TEFF to utilize a high frequency table.

To increase testing capability, the TEFF acquired two high frequency piezoelectric shaker tables to use in high cycle fatigue testing. The shaker tables were purchased from a Florida based company which did not supply adequate technical data. The tables are currently in use, but the unknown system parameters due to the lack of technical data makes it difficult to use the tables to their fullest potential. Therefore, a material characterization and Finite Element Model (FEM) is necessary to completely identify the material properties and modal characteristics.

A FEM is required to identify the resonant frequencies of the shaker table assembly to avoid shattering the expensive piezoelectric crystals, and to predict behavior of test articles added to the table before testing. A complete FEM will save AFRL money

and time, allowing the TEFF to operate more effectively and efficiently. The objective of this thesis work is to create and validate a FEM for one of the TEFF's piezoelectric shaker tables. This task requires a thorough understanding of the theory, operation, and mechanics of a piezoelectric shaker table.

Background

Fatigue is a difficult failure mechanism to detect in materials which occurs when a component is weakened by repeated alternating load and unload cycles (Bhat and Patibandla, 2011:204). The repetition produces localized damage in the form of cracks which propagate and grow as the load is repeatedly applied and removed (Bhat and Patibandla, 2011:204). This type of failure occurs at load levels that produce stress which is much lower than the material's yield strength. Fatigue failure initiates from microscopic cracks that grow to a critical size, and therefore generally occurs without warning, and results in catastrophic material failure (Bhat and Patibandla, 2011:204).

Fatigue has frequently been a cause in failure of man-made machines, but it was not realized or investigated until the industrial revolution. During this boom of manufacturing growth, a particularly devastating railway disaster in 1842 triggered William John Rankine of British Railway Vehicles to exam the broken axle of a locomotive (Bhat and Patibandla, 2011:203). Rankine's examination determined the locomotive axle had failed due to a brittle crack through its diameter (Bhat and Patibandla, 2011:203). This work was continued by August Wöhler who further investigated the effects of cyclic loading on locomotive axles and developed the stress-rpm (S-N) diagram for estimating fatigue life (Bhat and Patibandla, 2011:203).

Following Wöhler, Johann Bauschinger first published data on the cyclic stress-strain behavior of materials in 1886 (Schūtz, 1996:265-267). As the 19th century drew to a close these advancements in understanding began to be implemented in design and development, but the heightened production rates of World War II showed that the understanding and criticality of fatigue failure analysis was not complete. Large scale failure of welds on Liberty Ships quickly produced for the war renewed interest in fatigue failure and prompted future reports on the number of fatigue related catastrophes (Bhat and Patibandla, 2011:204). One report detailed results from several years of aircraft failure investigations published in 1981 showed fatigue was a leading cause of aircraft failure and death (Campbell, 1981:182). The publication also indicated for fixed wing aircraft, a frequent cause of failure was engine component fatigue (Campbell, 1981:182).

Findings such as these stressed the need for organizations, especially those operating aircraft, to place more emphasis on proactive fatigue research and testing. As an organization dependent on aircraft, the United States Air Force (USAF) recognized that fatigue research, analysis, and testing is extremely important for maintaining aircraft, and ensuring the safety of its aircrews. To address the ongoing need for research and testing, the USAF established the AFRL Turbine Engine Fatigue Facility as the lead office for turbine engine component fatigue. As the primary source of fatigue research, the TEFF conducts tests to quantify life expectancy of components subjected to anticipated loads and operating conditions. Data from these tests is analyzed to determine when critical system components should be replaced to avoid fatigue and catastrophic failures like those documented by Campbell. However, despite the ongoing

drive towards prevention, component failures still occur, and the TEFF is tasked to evaluate the cause of these failures in fielded systems so they can be corrected.

To conduct this research, the TEFF has traditionally used electrodynamic shakers as the primary mechanism for applying cyclic loads to engine components. An electrodynamic shaker, shown in Figure 1, resembles a common loudspeaker, but is more robust for vibration testing (Lang and Snyder, 2001:2). They operate by passing current through a coil suspended in a radial magnetic field to produce an axial force proportional to the current (Lang and Snyder, 2001:2). For large load capacity shakers, these tables usually operate at a frequency in the 5 Hz to 3,000 Hz range, where the high frequency performance is limited by the "coil mode" resonance (Lang and Snyder, 2001:10). These electrodynamic shaker tables have typically been excellent for cyclic load tests, with the limited frequency range being their main weakness. To compensate for the frequency limit while retaining forcing capability, and to increase frequency range capabilities, the TEFF chose piezoelectric shakers as an alternative test bed to electrodynamic shakers.

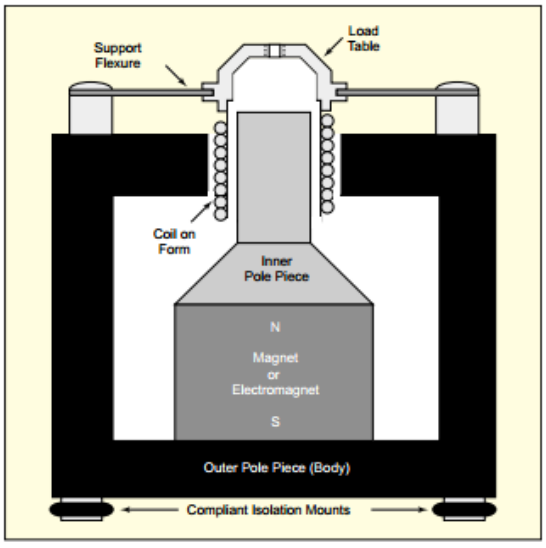

Figure 1. Electrodynamic Shaker Structure (Lang and Snyder, 2001:2)

Piezoelectric shaker tables, like their electrodynamic counterparts, produce a mechanical displacement when an electrical field is applied. However, rather than using hydraulics or magnets, piezoelectric shakers produce mechanical motion using piezoelectric ceramic materials. These materials have microscopic properties that cause the crystal ceramic to deflect when an electrical field is applied (Jordan and Ounaies, 2001:1). To achieve this effect Lead, Zirconium, and Titanium mixed oxides (PZT) are combined to create a ceramic electro-active piezoelectric material (Pickelmann, 2010:7). The piezo-ceramics are often referred to as piezoelectric crystals because they form a solid with ordered atoms which follow the perovskite structure shown in Figure 2 (Jordan and Ounaies, 2001:2).

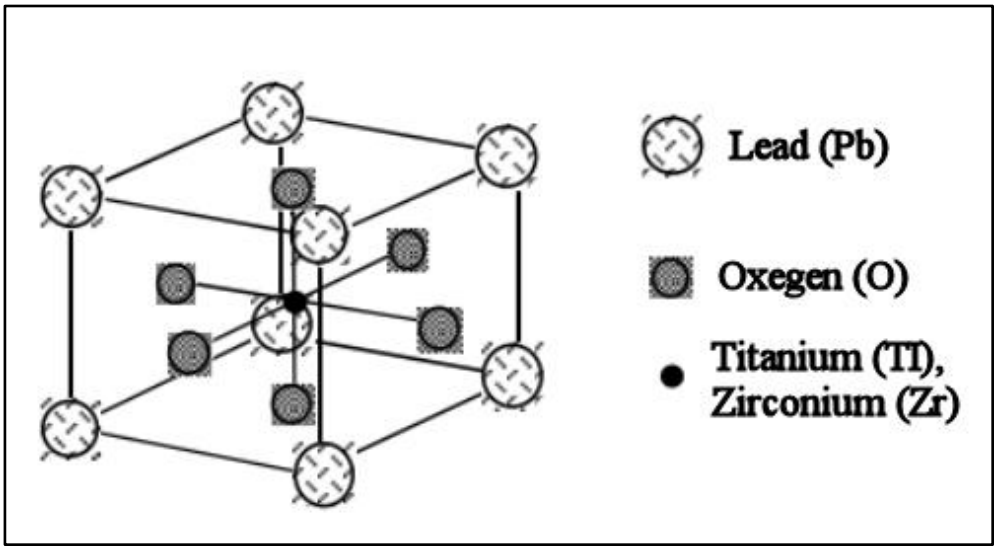

Figure 2. Perovskite Crystal Structure of PZT Ceramics (Jordan and Ounaies, 2001:2)

The central octahedral B-site of the perovskite structure is occupied by Titanium and Zirconium in a PZT ceramic (Jordan and Ounaies, 2001:3). This site is often treated

with a dopant to tailor the properties of the piezoelectric material (Jordan and Ounaies, 2001:3). Specifically, adding a dopant to this site increases the piezoelectric charge coefficients which are constants of proportionality between the applied electrical field and the resulting strain (Jordan and Ounaies, 2001:10). Increasing these coefficients makes the piezoelectric shakers suitable for higher frequency testing where electrodynamic shakers are limited. Because of the tailored PZT properties, piezoelectric shakers are able to produce larger accelerations at high frequencies than electrodynamic shakers (Payne et al, 2010:373). Producing large accelerations with electrodynamic shakers is also possible, but cost prohibitive because large amplifiers and cooling systems are required (Payne et al, 2010:373). However, these larger accelerations are possible with piezoelectric shakers at high frequency because the B-site dopant changes the properties of the PZT in such a way that it requires smaller amplifiers and generates less heat than electrodynamic shakers.

PZT ceramics are the most widely used piezoelectric material because of their high dielectric and piezoelectric properties (Jordan and Ounaies, 2001:2). They are utilized in actuators, such as the shaker table system shown in Figure 3, by stacking them in series with a copper electrode to create an electrical circuit shown in Figure 4 (Moheimani and Fleming, 2006:14). By stacking the crystals, the amount of longitudinal displacement produced is proportional not only to the voltage applied, but also to the number of crystals in the stack (Pickelmann, 2010:9).

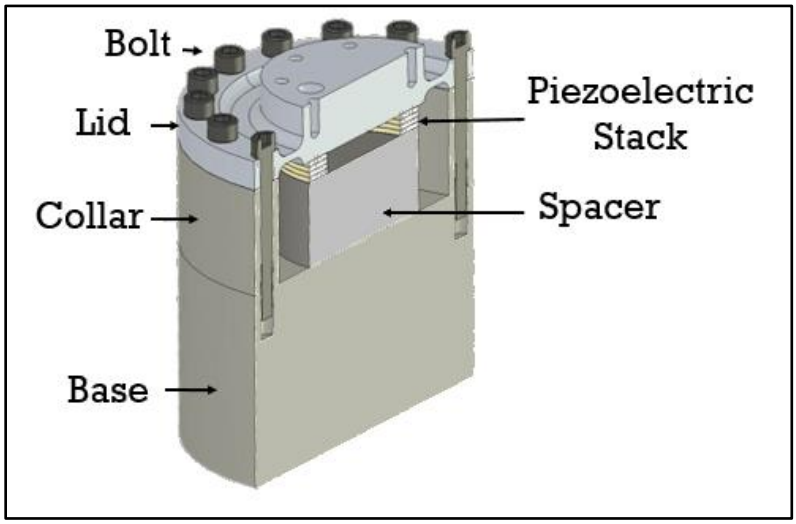

Figure 3. Piezoelectric Shaker Cross Section

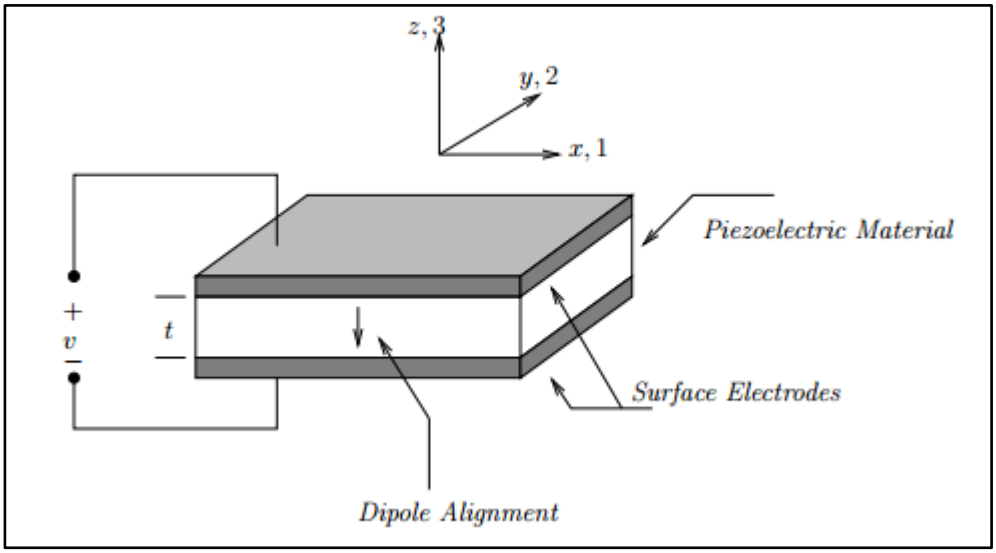

Figure 4. Piezoelectric Stack Electrical Circuit (Moheimani and Fleming, 2006:14)

The proportional relationship between applied electric field and mechanical strain in a PZT is linear, and is determined by a material property called the charge coefficient, $d_{ij,}$ which has units of distance per volt applied. When voltage is applied to a piezoelectric crystal in the direction of the poling voltage, the crystal will increase in

length, and decrease in diameter (Moheimani and Fleming, 2006:13). If the voltage is applied with opposite polarity of the poling voltage, the crystal will decrease in length and increase in diameter (Moheimani and Fleming, 2006:13). When an alternating voltage is applied, a crystal will expand and contract cyclically, as shown in Figure 5, at a frequency equivalent to the applied voltage (Moheimani and Fleming, 2006:13). When operated with alternating voltage, the piezoelectric material converts electrical energy into mechanical energy, and functions as an actuator (Moheimani and Fleming, 2006:13).

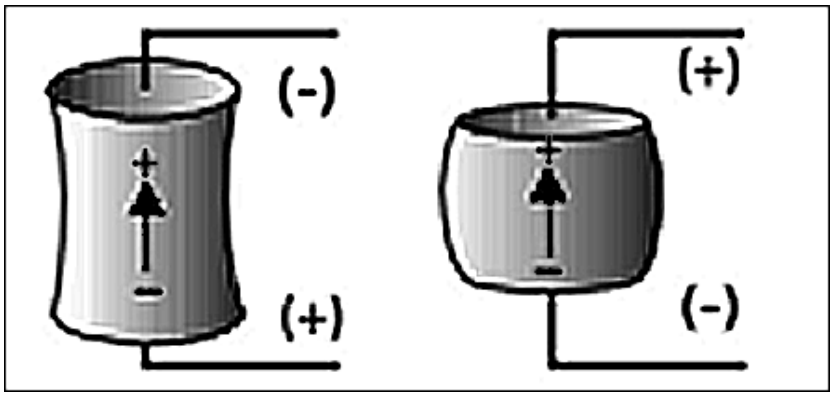

Figure 5. Piezoelectric Crystal Reaction to Alternating Voltage (Moheimani and Fleming, 2006:13)

The TEFF acquired PZT piezoelectric tables to conduct high frequency testing. The TEFF operates these shaker tables with three piezoelectric crystal stacking configurations, which depend on the amount of displacement, acceleration, and force required for a test. A four crystal stack which uses a spacer to bring the crystals in contact with the shaker lid is the most commonly used arrangement, but the TEFF also has enough crystals to create ten and twenty stack arrangements as required. The TEFF piezoelectric shakers are typically operated in the 100 Hz to 30 kHz range, but the signal

generator used to operate the shakers is capable of driving them at frequencies up to 50 kHz.

The piezoelectric shaker tables have reduced the time required to accumulate one billion cycles from days to 20 hours, which has significantly increased the TEFF capabilities for high cycle fatigue testing (Scott-Emuakpor et al, 2012). However, the crystals used in the devices are fragile and expensive, and it is necessary to characterize the system they are used in to avoid resonant frequencies, which can cause the crystals to shatter. This characterization is necessary because the shakers were provided without adequate technical. Modal characterization of the AFRL piezoelectric shaker table system is the primary purpose of the mechanical model developed later in this document.

Research Objectives

The specific objective is to produce an experimentally validated FEM of the shaker table, which the TEFF can use to plan and execute future tests. The steps (objectives) which must be completed to create and validate a working FEM for the piezoelectric shaker table are:

(1) Produce initial simplified mechanical model solution
(2) Use optical scanner to acquire point cloud data of shaker table components
(3) Create a solid model of the shaker table components
(4) Import the solid model into FEM package (ANSYS)
(5) Conduct ping tests to obtain response data
(6) Compare component FEM to experimental data
(7) Adjust component model parameters to match experimental data
(8) Repeat steps 5 & 6 until the FEM model agrees closely with experimental data
(9) Conduct experiments on the shaker table system to obtain response data
(10) Compare simplified models and system FEM to experimental data
(11) Validate the FEM

The preliminary steps promote a deeper understanding of the theory and mechanics of the shaker table system so the FEM produced in the remaining steps will more accurately reflect the true physical system. These initial steps will provide a means for knowledgeable review of results produced by the FEM rather than a blind acceptance of accuracy. The remaining steps will produce the FEM and provide a means for validating the results. Overall, the outlined steps will completely satisfy AFRL's requirement.

Assumptions/Limitations

The work conducted in this thesis research was guided by three major assumptions. First, a simplified model was created as an initial investigation into the shaker table vibration response. This model was a simplified one-dimensional model of a more complex continuous three-dimensional problem. The Equation of Motion (EOM) derived from this model is for a discrete SDOF system, yielding a single resonant frequency. In reality, an infinite number of natural frequencies exist for this continuous system. For this reason, there are limitations in the simplified model, but these limits are known, and it was assumed the simplified model still provides valuable insight regarding the system characteristics.

Second, the mechanical model of the TEFF piezoelectric shaker table is a three dimensional analysis problem that is very complex, however, the overall response of the shaker table is determined not only by the mechanical response, but also by a coupled electrical response the piezoelectric crystals produce. The electro-mechanical coupling is a more complex problem not investigated in this research work. It was assumed the

mechanical response would capture the majority of the system modes, and the FEM produced of the shaker table was designed to predict the mechanical response of the system, leaving the coupling effects for future work.

Lastly, the TEFF can operate the shaker tables using three different piezoelectric crystal stacking configurations. However, the focus of this research was limited to the four crystal stack arrangement because the relationship between number of crystals in the stack and strain is linear. It was assumed the ten and twenty stack configurations are materially the same as the four stack configuration, and a validated FEM could be scaled to predict the modal characteristics of the larger stack arrangements.

Summary

The main purpose of this chapter was to introduce the reader to the Turbine Engine Fatigue Facility piezoelectric shaker table and outline the lack of technical data that is the main motivation for this thesis work. It provided context to stress the importance of fatigue research and how shaker tables are important to the field. The topic of piezoelectric material was introduced, and their use in making high frequency shaker tables was described. It pointed out piezoelectric shaker tables are well suited and important to high frequency fatigue research, and described how these shakers work. A lack of technical data for these shakers was emphasized as a root cause of the gap in knowledge, and what makes it difficult to maximize their use. Finally, a complete material characterization and Finite Element Model (FEM) was proposed to fully characterize the shaker table and complete the technical data package.

II. Literature Review

Chapter Overview

The purpose of this chapter is to provide a theoretical context for the work completed in this research. It is also intended to provide a survey of relevant research completed in the field of piezoelectric modeling and characterization. There are multiple operating principles and theories underlying this effort, and an understanding of them was critical to meeting the objectives.

This chapter will briefly outline a small section of vibration theory used to generate a simplified mechanical model of the piezoelectric shaker table system. In addition, it will provide details on the theory of finite element simulations. Operational use of the 3D scanning device, laser vibrometer, and neoprene isolation pad will also be discussed. This chapter will close with an overview and survey of work completed in the field of shaker table modal characterization.

Theoretical Development

Vibration

Vibration theory was important to this work and the simplified model analysis because the basic function of a shaker table is to induce oscillatory force into an object. This theory has been developed over many years to address the fact every material, system, component, etc., responds to initial, discrete or continuous excitations (Meirovitch, 2010). The undamped vibratory response of a system can produce unwanted and catastrophic effects for the object under consideration. An example of the

catastrophic effect of vibrations is the Tacoma Narrows Bridge, which failed when excited by wind at the structural resonant frequency (Meirovitch & Ghosh, 1987).

Applying vibration theory begins by evaluating a system to determine its constraints, components, and material properties to create a mechanical model. This model can then be analyzed using several different techniques to produce a Differential Equation of Motion (DEOM), which describes how the system responds to an input force. A short list of the analytical mechanic techniques used to produce an EOM include; LaGrange (energy method), Extended Hamiltonian Principle (energy method), Newtonian (vectorial mechanics), etc (Meirovitch, 2010:1). For this research, a vectorial mechanics approach was used to produce the simplified model.

The vectorial mechanics approach consists of generating a Free Body Diagram (FBD) of the mechanical system by identifying the external forces acting on the discrete masses of the system. Each of the system masses is characterized by one or more coordinate systems, termed Degrees of Freedom (DOF), which represent the movement of the mass. The forces for each mass are summed and equated to a Kinetic Diagram (KD), which describes the motion of the system, as shown in Equation (1). The equation produced using the approach is consistent with Newton's second law of motion F=Ma (Meirovitch, 2010:2-6).

$$\sum F = F(t) - kx - c\dot{x} - Mg = M\ddot{x} \tag{1}$$

Where *F(t)* is *input force*, *k* is *stiffness*, *c* is *damping*, *M* is *mass*, *g* is *acceleration due to gravity*, *x* is *displacement*, $\dot{x}$ is *velocity*, and $\ddot{x}$ is *acceleration*.

The EOM shown in Equation (1), can be further simplified to eliminate the gravity terms by considering the motion about an equilibrium position where the system components are allowed to stretch based on the weight. Using a coordinate system in which the variable y represents the vertical displacement from the stretched (equilibrium) position, the difference between the *y* (stretched) and *x* (un-stretched) displacement is $y - x = \delta$. The derivatives of this relationship, $\dot{x} = \dot{y}$ and $\ddot{x} = \ddot{y}$, allow a change in variables from the unstretched to the stretched coordinate system. The force applied to displace the system to this equilibrium position is equal to the stiffness times the displacement, $F = mg = k\delta$. Substituting the force and displacement relationships into Equation (1) yields the second order linear differenetial EOM about the equilibrium position.

$$M\ddot{y} + c\dot{y} + ky = F(t) \tag{2}$$

Equation (2) represents an assemblage of discrete components which act together based on the parameters of the equation to describe the systems motion. The equation of motion must characterize the discrete components in order to be solved. Equation (2) shows there are three discrete components based on their proportional relationship to accelerations ($\ddot{x}$), velocities ($\dot{x}$), or displacements (x) (Meirovitch, 2010:23). The first type, masses (m), are components proportional to acceleration, which store and release kinetic energy through translational motion (Meirovitch, 2010:26). The second type, viscous dampers (c), are proportional to velocity, which dissipate energy (Meirovitch, 2010:25). These components produce forces and are characterized by physical

phenomenon such as friction, air resistance, electromagnetic forces, etc. The third type, helical springs (k), are proportional to displacement, which store and release potential energy (Meirovitch, 2010:23). These components are characterized by material properties that determine their elasticity, such as Young's modulus, Poisson's ratio, and density.

Solutions to Equation (2) take different forms based on the applied excitation F(t). For an undamped SDOF system with constant coefficients and non-zero forcing function, the solution to the DEOM has two parts. The first part is called the homogeneous solution (transient), and is found by setting the EOM equal to zero and solving a characteristic equation , $s^2 + \omega_n^2 = 0$, where $\omega_n = \sqrt{k/M}$ (Meirovitch, 2010:109-148). The characteristic roots are $s = \pm i\omega$, and the transient solution of a system with two repeated imaginary roots has the form shown in Equation (3). The solution to a homogeneous differential equation requires initial displacement and velocity of the system be set equal to Equation (4) and its derivative, respectively, to determine the constants of integration and ensure the solution matches the initial conditions of the system (Meirovitch, 2010:83).

The second part of the solution is called the particular solution (steady state) and it is computed by assuming a solution to the differential equation of the form shown in Equation (3) (Meirovitch, 2010:109-148). The assumed solution and its derivatives, shown in Equation (4) thru Equation (6), are substituted into the EOM and the sine and cosine function coefficients are equated to determine the constants of integration shown in Equation (7). The constants of integration are used to completely specify the total

solution, shown in Equation (8), which is computed by equating the initial conditions to the assumed solution and solving a system of equations.

$$y_h(t) = C_1 \cos \omega t + C_2 \sin \omega t \tag{3}$$

$$y_p(t) = D_1 \cos \omega t + D_2 \sin \omega t \tag{4}$$

$$\dot{y}_p(t) = -D_1 \sin \omega t + D_2 \cos \omega t \tag{5}$$

$$\ddot{y}_p(t) = -D_1 \cos \omega t - D_2 \sin \omega t \tag{6}$$

$$\omega^2(-D_1 \cos \omega t - D_2 \sin \omega t) + \omega_n^2(D_1 \cos \omega t + D_2 \sin \omega t) = \omega_n^2 A \sin \omega t \tag{7}$$

$$y_p(t) = AG(\omega) \sin \omega t = \frac{A}{1-\left(\frac{\omega}{\omega_n}\right)^2} \sin \omega t \tag{8}$$

Where y_h is *the EOM homogeneous solution*, y_p is *the EOM particular solution*, $\dot{y}_p$ is *EOM particular solution velocity*, $\ddot{y}_p$ is *EOM particular solution acceleration*, ω is *driving frequency*, ω_n is *natural frequency*, C_1 & C_2 are *constants of integration*, D_1 & D_2 are *constants of integration*, A is *excitation amplitude*, and $G(\omega)$ is *the frequency response function*.

Vibration theory presented assumes the system responds linearly to inputs and can therefore be characterized as a Linear Time Invariant (LTI) system. Because the system is LTI, the principal of linear superposition can be applied to combine the transient and steady state solutions together into a total solution, which represents the complete motion of the system to the applied external excitations (Meirovitch, 2010:53-57). Further

details and specific derivation of the EOM for the shaker table system will be shown Chapter III of this research.

Optical 3D Scanner

The Advanced Topometric Sensor (ATOS) used to complete 3D scans of the shaker table components in this research was manufactured by Gesellschaft für Optische Messtechnik (GOM). This system projects light patterns onto an object and measures the reflected light using two cameras to triangulate three-dimensional points in space representing the object's surface. To capture the entire surface of an object the system employs a 360-degree rotating table to record multiple sets of data, which are combined into a single global point cloud using photogrammetry (Rhoades, 2011:11). These point clouds are then post-processed using GOM's software, and exported into a Computer Aided Design (CAD) program of choice to create a 3D solid model.

The ATOS system supports multiple lens configurations with varying camera focal lengths to decrease measurement volume and increase accuracy of the system (Rhoades, 2011:12). Typical measurement volumes for the ATOS system are 90 mm, 120 mm, 250 mm, and 500 mm. The 120 mm volume lens (120mm x 108 mm x 95 mm) was used to acquire point cloud data in this work. Because the ATOS system uses triangulation to determine the location of points, the geometry of its components is very important, and a system calibration is required when lenses are changed. The calibration is accomplished using a manufacturer provided board, which has a printed pattern of known dimensions. The pattern is scanned, and used to determine the angles between the projectors and cameras when the ATOS systems software built-in calibration routines are used (Rhoades, 2011:29).

The light pattern projected by the ATOS system onto an object is a white stripe used to illuminate the objects surface (Rhoades, 2011:32). An image of the pattern is captured containing data representing the point locations based on distortion of the light when viewed from multiple angles (Rhoades, 2011:29). Multiple stripe patterns are projected onto the surface to fully capture the geometry, and the point data is stored in a gray coded binary format (Rhoades, 2011:32). The captured images from all the phase shifted patterns are then used in conjunction with the system's geometry to determine point coordinates through triangulation, as shown in Figure 6.

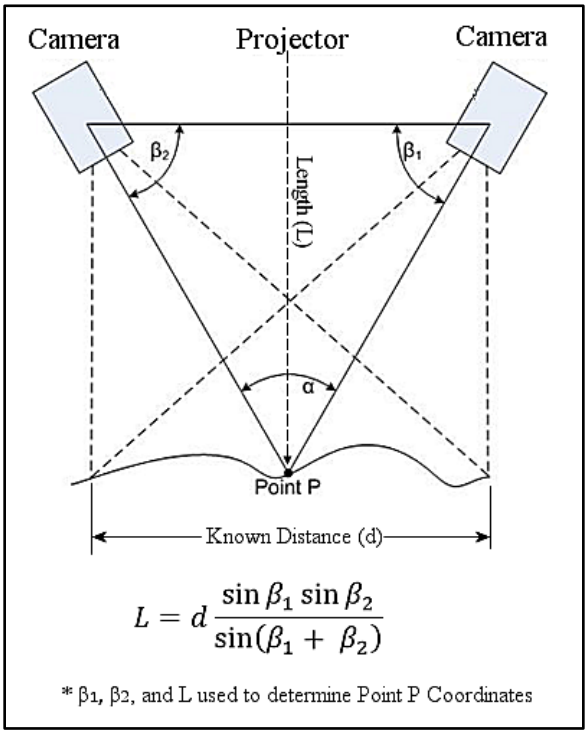

Figure 6. 3D Scanner Triangulation of a Point (Rhoades, 2011:30)

The ATOS system scans multiple sets of these images from different perspectives around the object by moving the object on a rotation table. To generate a full 360-degree

point cloud scan, the local coordinates are combined into a global coordinate system using photogrammetry (Rhoades, 2011:35). For the system to use photogrammetry, its positon relative to the object being scanned must be known. This orientation is accomplished using a bundling adjustment algorithm developed by Dirk Bergmann (Rhoades, 2011:35). His algorithm uses reference points attached to the surface, which are detected during the scans. The reference point coordinates are determined in the first scan, and each successive scan must include three reference points from the first scan to triangulate the system positon (Rhoades, 2011:36). Overall, the physical geometry of the systems projector and cameras is used in conjunction with the reference points to fully define a global data point. A visual representation of this process is shown in Figure 7.

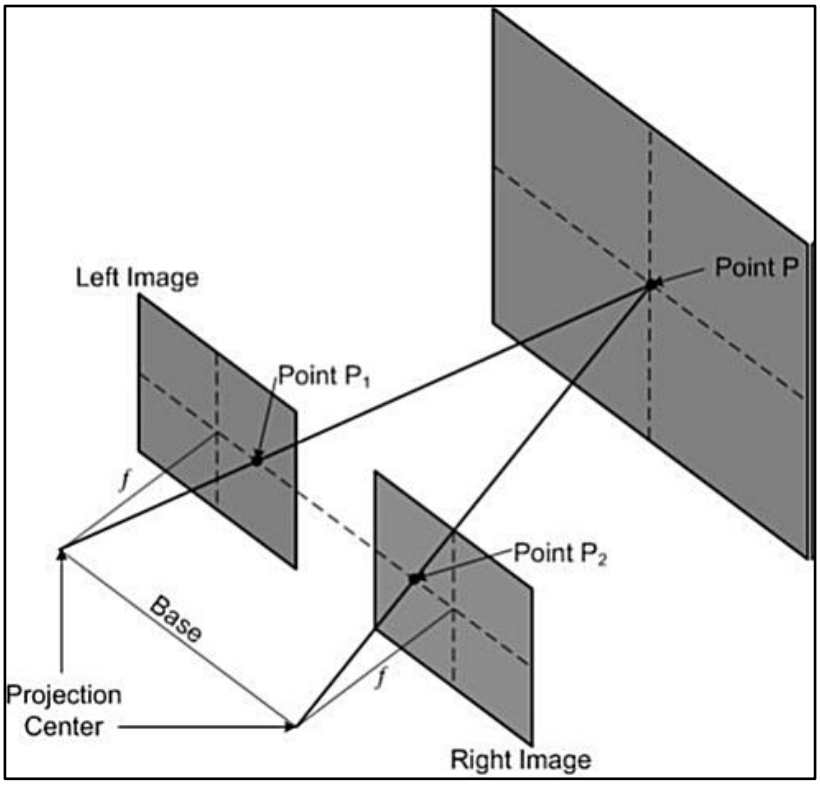

Figure 7. Photogrammetry Center of Projection (Rhoades, 2011:25)

After a scan is completed, the GOM software is used to post-process the point cloud data. Supports and other data not needed for the solid model are removed by highlighting the data and deleting the generated points. The point cloud data can be used to reorient the global coordinates, by selecting three reference points on a surface to define each coordinate plane, before exporting the image to a CAD 3D modeling system.

Isolation Pad

Isolation pads are used in industrial engineering to prevent equipment vibrations from entering into the surrounding environment. However, because of their vibration isolation properties, they can also be used in vibration fatigue testing to approximate support conditions which allow a test object to move freely in all degrees of freedom, a state known as a free-free boundary. Transmissibility and isolation efficiency are the two primary mechanical properties of an isolator. The transmissibility of the isolation pad is defined as the inverse ratio of the disturbance frequency to the natural frequency of the isolation pad, as shown in Equation (9) (D'Antonio, 2010:3). The isolation efficiency, shown in Equation (10), is a function of transmissibility (D'Antonio, 2010:3).

$$T_{iso} = \frac{1}{\left(\frac{\omega_d}{\omega_n}\right) - 1} \tag{9}$$

$$IE = 100(1 - T_{iso}) \tag{10}$$

Where T_{iso} is *transmissibility of the isolator,* ω_d is *driving frequency,* ω_n is n*atural frequency*, and *IE* is *isolation efficiency*.

Equation (10) and Equation (9) show isolation efficiency is maximized by increasing the ratio of disturbance to support natural frequency. The isolation capability of these pads begins when the ratio exceeds a value of 4:1, and 90% or better isolation efficiency is obtained at ratios of 4:1 or greater. (D'Antonio, 2010:3). When using these isolation pads to conduct experimental modal analysis, a ratio as high as 10:1 is desired to ensure a 99% isolation efficiency (Carne et al, 2007:10). Understanding these operating principles allows isolation pads, such as the Fabreeka's Fabcel 25 neoprene pad used for this thesis work, to be employed for approximating free-free boundary conditions when the test object natural frequency is at least four times greater than the isolation pad natural frequency.

Laser Vibrometer

The laser vibrometers used for this research detect ohject velocity and displacement at a fixed point using the Doppler-effect. A light signal of known wavelength is focused on an object and when the object moves, the light signal experiences a frequency shift, which is characterized by Equation (11) (Polytec, n.d).

$$f_d = \frac{2v}{\lambda} \tag{11}$$

Where f_d is *Doppler effect* f*requency shift*, v is *velocity*, and λ is *wavelength*.

Equation (11) can be used to determine displacement and velocity when the wavelength is known, and the frequency shift is measured. To measure the frequency shift, laser vibrometers use a concept known as optical interference (interferometry),

which determines the path length difference between two overlapped beams of variable intensity light (Polytec, n.d).

The two light signals used in interferometry are generated by a single laser, and are split into a reference and a measurement beam, as shown in Figure 8 (Polytec, n.d). One portion of the reference beam is reflected through a Bragg cell, which shifts the frequency 40 MHz for later comparisons (Polytec, n.d.). The measurement beam is passed through another beam splitter, and focused on the object before its reflected signal returns to the vibrometer and is passed through another beam splitter with the reference signal. These signals are directed onto a detector, which generates dark and bright patterns based on the magnitude and direction of the displacement. The direction is determined based on whether the detector receives a dark or bright signal when the reference and measurement signals are combined with the Bragg signal (Polytec, n.d.).

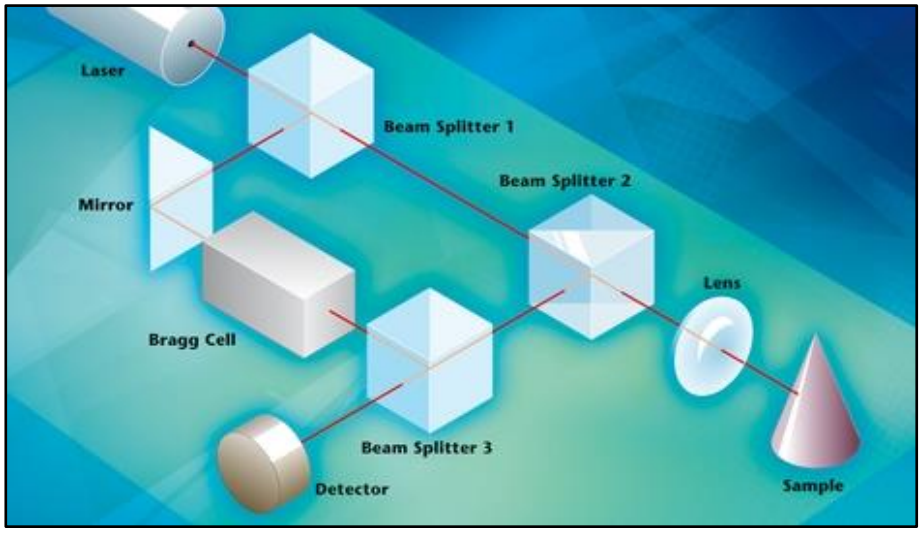

Figure 8. Laser-Doppler Vibrometer Core (Polytec, n.d)

Laser vibrometers of this type are used to measure either displacement or velocity. However, because higher velocities are generated at small displacements for

high frequency harmonic vibrations, it is best to measure displacement at low frequencies and velocity at higher frequencies (Polytec, n.d.). For this research, both displacement and velocity response was measured using a vibrometer, but velocity data was used as the primary method of comparison with other data because piezoelectric shakers operate at high frequencies.

Finite Element Analysis

The foundation of this research was to produce a model, which could reasonably predict the modal characteristics of a piezoelectric shaker table. The chosen modeling approach to predict these characteristics was a Finite Element Analysis (FEA) because this type of modeling is well suited for complex structures for which analytical solutions do not exist. FEA modeling allows the system to be evaluated by entering geometric and material properties, and programming a computer to discretize the system into a prescribed number of sections, known as elements, based on the specified section sizing (mesh) and shape (element type). The properties of these elements are stored in matrices, which represent the local mass, damping, and stiffness characteristics of the elements. These matrices are assembled into global representations to produce and solve the matrix equation of motion for the structure, which is shown in Equation (12) (Rieger, n.d.:2).

$$[M]\{\ddot{u}\} + [C]\{\dot{u}\} + [K]\{u\} = \{F\} \tag{12}$$

Where *[M]* is *the mass matrix, {ü}* is *acceleration matrix, [C]* is *the damping matrix, {u̇}* is *velocity matrix, [K]* is *the stiffness matrix, {u}* is *displacement matrix,* and *{F}* is *the force matrix.*

To determine the modal characteristics of the system the free vibration response is needed, and therefore Equation (12) is reduced to the undamped homogeneous matrix equation by setting the damping matrix [C] and force matrix {F} equal to zero, as shown in Equation (13) (Rieger, n.d.:2). Without the damping matrix, all the connection points of finite element sections, called nodes, move in phase at the same natural frequency (Cook et al, 2002:384). The free vibration response is described by the nodal amplitudes, captured in a matrix, which vary sinusoidally in time relative to static equilibrium displacements, as shown in Equation (14) (Cook et al, 2002:384-385). The associated nodal accelerations, shown in Equation (15), are found by taking two derivatives of Equation (14) with respect to time. Substituting Equation (14) and Equation (15) into Equation (16) yields a relationship which describes the undamped free vibration and is the form of the eigenproblem, shown in Equation (13) (Cook et al, 2002:385). The solution to the eigenproblem provides the natural frequencies (eigenvalues) and mode shapes (eigenvectors) of the system (Rieger, n.d.:2).

$$[M]\{\ddot{u}\} + [K]\{u\} = 0 \tag{13}$$

$$\{u\} = \{\bar{u}\} \sin \omega t \tag{14}$$

$$\{\ddot{u}\} = -\omega^2\{\bar{u}\} \sin \omega t \tag{15}$$

$$([K] - \omega^2[M])\{\bar{u}\} = 0 \tag{16}$$

Where *{ū}* is *the displacement amplitude matrix*, *t* is *time*, and *ω* is *the driving frequency*.

The eigenproblem solution to a system having multiple nodes free to move in numerous directions must be solved iteratively. Finite element software available today employs many solution algorithms, but due to reduced storage needs and computational time, the Lanczos method is a leading algorithm. The Lanczos method replaces the single column displacement matrix with a matrix that that spans the entire eigenproblem and uses sequential inverse iteration to determine the eigenvalues and eigenvectors. Obtaining the system response, natural frequency, and mode shapes is the primary function of a finite element modal analysis. The solution process outlined above was used by the ANSYS Workbench Mechanical solver when a modal analysis was conducted on the piezoelectric shaker table system studied in this research.

FEA is an excellent standalone tool that can be used to characterize complex systems, but modal testing is often desired to complement the finite element analysis, which can be used to obtain natural frequencies through direct measurement (Rieger, n.d.:2). Results from modal testing can be used to confirm FEA natural frequency predictions and the natural mode test data may also be used to determine the modal mass and stiffness matrix of the structure for an FEA (Rieger, n.d.:2).

Relevant Research

Piezoelectric materials have been in various stages of use since their discovery in the 19th century. Material developments in the mid twentieth century opened the door for more wide spread use, and the creation of a stable, highly sensitive Lead Zirconate Titanate (PZT) ceramic has expanded their use. Exhaustive studies have been conducted on these materials, and the constitutive equations shown in Equation (17) and Equation

(18) have been developed to describe their behavior (Piefort & Preumont, n.d.:2). These constitutive equations for piezoelectric materials are similar to their mechanical counterparts, and a comparison of their definition is shown in Table 1.

$$\{T\} = [c^E]\{S\} - [e]^T\{E\} \quad (17)$$

$$\{D\} = [e]\{S\} - [e^S]\{E\} \quad (18)$$

Where *{T}* is *the stress matrix*, *$[c^E]$* is *the piezo material elasticity constants matrix*, *{S}* is *the strain matrix*, *[e]* is *the piezoelectric coupling coefficients matrix*, *{E}* is *the electric field matrix*, *{D}* is *the electric displacement matrix*, and *$[e^S]$* is *the piezoelectric coupling coefficients matrix at constant strain*.

Table 1. Electromechanical Analogy (Piefort & Preumont, n.d.:2)

Mechanical		**Electrical**	
Force	{F}	Charge	σ
Displacement	{u}	Voltage	ϕ
Stress	{T}	Electric Displacement	{D}
Strain	{S}	Electric Field	{E}

The research conducted on these materials has been primarily to characterize their material properties. Extensive literature exists on the study and characterization of the multitude of piezoelectric materials commercially available. A study presented by several researchers from the University of Hawaii in 2006 on the topic of vibration control using piezoelectric materials characterized the stiffness matrix, piezoelectric matrix, dielectric matrix, and piezoelectric charge coefficient matrix properties required for a full ANSYS finite element characterization of PZT-5A, the material used in AFRL's piezoelectric

shaker table (Uyema, M. et al, 2006:314-320). Although valuable for the final model, the piezoelectric matrix, dielectric matrix, and charge coefficient matrix properties were specifically related to the electrical response of the piezo material and were not relevant to this step of the research because only the mechanical relationships were modeled. However, the stiffness matrix data was used in the mechanical model, and the electrical matrices will be needed for future work on the final product, which will account for electromechanical coupling.

Additional work has been done in modeling piezoelectric actuators made almost wholly of piezoelectric material alone. These type of systems are typically employed at miniature scales to actuate systems that cannot use traditional actuation methods because of their size. These piezoelectric materials are used to produce the structure and actuate it, and they are often used with composite materials when additional structural integrity is required. Exhaustive studies have also been conducted on simple beam, disk, plate, and other standalone piezoelectric structures. Most of these studies include a finite element model of the piezoelectric system compared to experimental results. One study presented by two researchers covers multiple shapes and applications, but it still primarily focuses on the material properties of the piezoelectric material and does not address its use in a complex system like the piezoelectric shaker table operate by the TEFF (Piefort & Preumont, n.d.:5-16).

A research project presented by researchers from the Beijing Institute of Spacecraft Environment Engineering at the 14th International Congress on Sound and Vibration in 2007 accomplished almost the same objectives of this research, but the work was done with a traditional electrodynamic shaker instead of a piezoelectric shaker (Shu-

Hong et al, 2007:1-7). This research outlined a process similar to the one used in this work where the sub-components of the shaker were first evaluated, modeled, and tested to optimize the model shaker table model (Shu-Hong et al, 2007:1-7). The complete system was assembled and a finite element simulation was run for comparison with experimental data (Shu-Hong et al, 2007:1-7). This project determined the finite element model agreed with experimental data when this process was used, and the researchers concluded this modification process was practicable (Shu-Hong et al, 2007:1-7).

There have also been publications suggesting virtual shaker testing is a method for improving experimental vibration test performance (Ricci et al, 2009:1-5). Research presented in these publications indicates interaction between test items and test equipment is a critical issue because the test facility and test article often couple their response at frequencies of interest (Ricci et al, 2009:1-5). The conclusion of these publications is virtual finite element simulations closely representing the real test scenario can be run prior to physical tests to better plan and execute the actual tests (Ricci et al, 2009:1-5).

Overall, there is a wealth of related information and research available to support this thesis work. Many of the publications support the approach and reason for conducting the research while others provide some needed bit of information to begin the process. However, this work is relatively new because it is the first of its type in which piezoelectric crystals have been implemented into a more complex system to determine modal characteristics using a finite element simulation. This work will be extending the previous work highlighted in this chapter to a new level of complexity.

Summary

The research conducted in this thesis is based on many foundational theories and a great deal of previous research. The experimental tests conducted in this thesis required an understanding of optical 3D scanning theory, isolation pad theory, laser vibrometer operating principles, and the theory behind finite element analysis. In addition, the analysis conducted in this thesis also required an understanding of vibration theory. These topics were all discussed to the level needed for a required understanding of the work and results presented in this thesis.

This research was also described in context of previous work. Publications on relevant topics and their results were review and discussed. The contributions of the research contained in these publications to the current work was also highlighted. Overall, it was noted that while there are many contributing theories and research articles that this thesis relies on as a foundation, it is still a new endeavor that takes the previous work and extends it to an increased level of complexity.

III. Methodology

Chapter Overview

The primary goal of this research was to develop an analytical model of the piezoelectric shaker for AFRL to use when conducting high cycle fatigue tests. The purpose of creating the model was to identify the system resonant frequencies and system behavior during fatigue testing. The general approach used to achieve this goal was a combination of analysis and experimentation.

Prior to creating a finite element model, a preliminary model was created to investigate the shaker table characteristics. This model was a simple Single Degree of Freedom (SDOF) system used to stimulate a more thorough understanding of the shaker table system mechanics and characteristics so it could be modeled more accurately using finite element analysis software. It was also an easy way to quickly determine at least one natural frequency of interest, and to provide a good approximation of displacement amplitude, applied force, and maximum voltage.

Using the knowledge garnered from the simplified model, a finite element model of the shaker components was created and used to analytically determine the modal characteristics of each component. Experimental data was collected from the physical components using single point laser vibrometers. The analytic and experimental data sets were compared, and the model parameters were adjusted until the finite element data matched the experimental data. As a final step to validate the model, a comparison was made between a FEM of the complete system and experimental data.

Simplified Model Design

The piezoelectric shaker tables used by AFRL are composed of five main components: base, collar, spacer, piezoelectric stacks, and lid. To apply the modeling techniques and mathematics of classical vibration theory, a primary assumption was necessary to reduce the problem from three-dimensions to two-dimensions. It was assumed, due to symmetry, the shaker table mechanical model could be produced from an x-y plane cross section of the table. From this primary assumption, several subsequent assumptions were made regarding physical representations and dimensions of the shaker table components.

First, the shaker base is a large mass of stainless steel, which is rigid, and the lid is attached to the base through the collar with high strength bolts, as shown in Figure 9. Because the base is rigid and rests directly on the table, it is assumed to be a fixed rigid constraint. By extension, the collar is assumed to be a fixed rigid constraint.

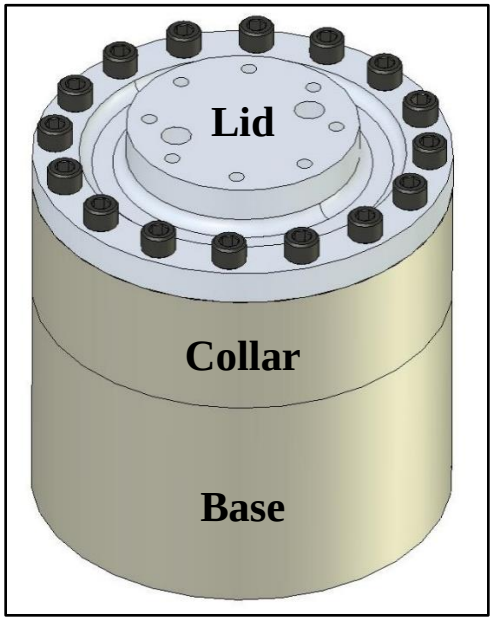

Figure 9. AFRL Piezoelectric Shaker Table

Second, the shaker lid, shown in Figure 10, is bolted to the base at the outer edge of the filleted groove in the lid. This point is assumed to represent a clamped end of a beam with length and height dimensions of the groove. The width of the beam was assumed to be equal to the height to obtain a square cross-section beam.

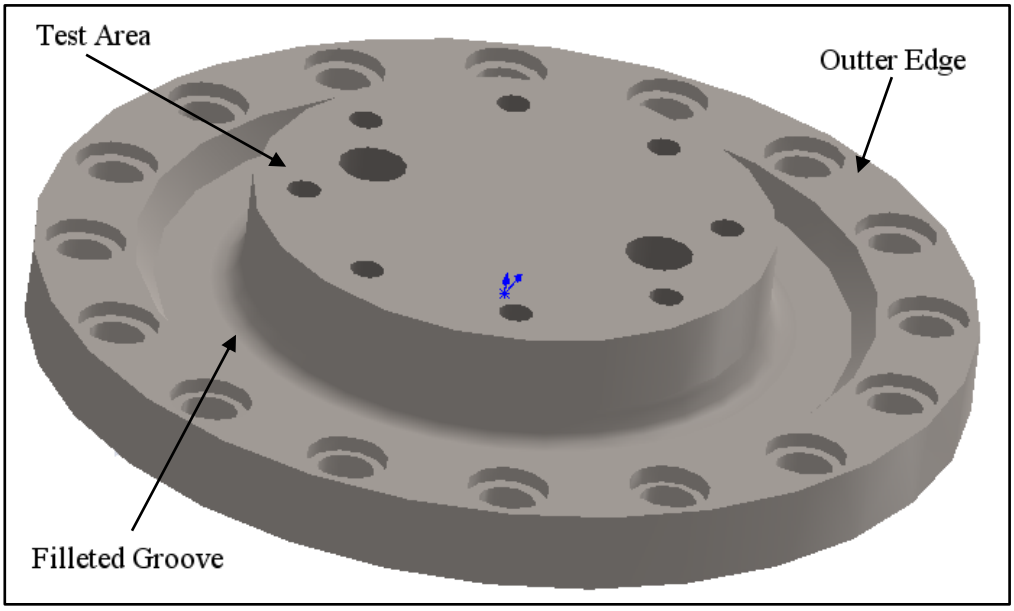

Figure 10. Shaker Lid Physical Characteristics

Third, the shaker lid test area is assumed to be a lumped mass clamped to the end of the beam structure of the lid groove. By assuming a lumped mass, the system can be modeled as a discrete instead of a continuous system. The lumped mass represents a SDOF, and is used to derive the equations of motion. The reduction of the problem to a SDOF through these simplifying assumptions results in a solution that admits a single natural frequency, while the system would realistically have an infinite number of natural frequencies. This was a known limitation of the simplified model, which was accepted

because of the models contribution to understanding of the system.

Finally, the piezoelectric stack is made of components which have an axial stiffness based on the cross-sectional area, length, and modulus of elasticity of the components. The stiffness of the stack is assumed to represent a spring with a spring constant equivalent to the axial stiffness of the piezoelectric stack.

Applying the assumptions outlined above, a two-dimensional mechanical model of the shaker table was developed and shown in Figure 11 below.

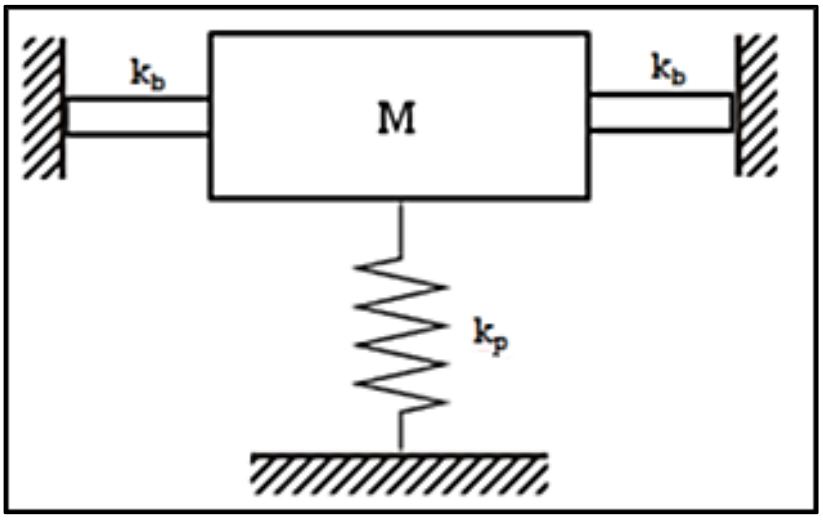

Figure 11. Simplified Piezoelectric Shaker Table Mechanical Model

The EOM for the mechanical model was found by applying Newton's Second Law. A FBD was constructed for the system lumped mass shown in Figure 12. The forces acting on the mass in the FBD were summed and equated to a KD describing the motion of the system. This method of equating FBD to KD is called the vectorial approach because it stems from Newton's Second Law, force equals mass times acceleration (Meirovitch, 2010:2).

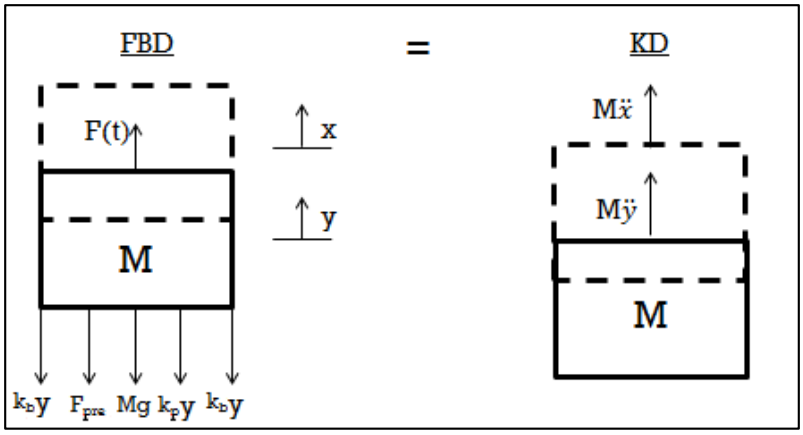

Figure 12. Simplified Piezoelectric Shaker Table FBD and KD

To define the forces applied to the mass, an equivalent representation of the beam stiffness acting in the vertical direction had to be determined. The beam was considered to be clamped at both ends with the end supporting the mass sagging under the weight and preload of the lid. Applying these interpretations, the equivalent beam stiffness in the vertical direction was found to be $k_b = \frac{12EI}{L^3}$ (Meirovitch, 2010:38). In addition to beam and piezo stack forces, the weight (Mg), forcing function F(t), and load applied to the lid by tightening the bolts (F_{pre}) were also represented in the model.

Using the generic force representation above, the EOM was determined by realizing there are two possible coordinate systems. Assigning *x* as the displacement about the non-equilibrium position, *y* as a displacement about the equilibrium position, and δ as the difference between *x* and *y*, the formula $x = y - \delta$ was derived to describe the relationship between the coordinate systems. A force is applied to move the system to the equilibrium position, and it is related to displacement by a spring constant through the equation $F = k\delta$. Using the *x*-*y* and force-displacement relationships and assigning a

sinusoidal forcing function to represent the electrical signal, the mechanics of the system can be used to obtain the EOM:

$$\ddot{y} + \omega_n^2 y = \omega_n^2 \, A \sin \omega t \tag{19}$$

Where $\ddot{y}$ is *acceleration*, ω_n is *natural frequency*, y is *displacement*, A is *excitation amplitude*, ω is *driving frequency*, and t is *time*.

To compute the displacement and frequency response of the shaker table mechanical model developed above, the solution to the differential EOM shown in Equation (19) had to be solved. The complete solution to an un-damped SDOF system with harmonic excitation contains a homogenous (transient) and particular (steady-state) solution. However, because the EOM is about the equilibrium point, the model has no initial displacement or velocity, solving the characteristic equation $s^2 + \omega_n^2 = 0$ resulted in a homogeneous solution $y_h(t) = 0$.

The particular solution was calculated by assuming a form of the solution $y_h(t) = C_1 \cos\omega t + C_2 \sin\omega t$. Substituting the assumed solution and its first and second derivatives into the EOM, then equating the coefficients of the sine and cosine terms yields a system of equations, which were solved to compute the complete particular solution:

$$y_p(t) = AG(\omega) \sin \omega t = \frac{A}{1-\left(\frac{\omega}{\omega_n}\right)^2} \sin \omega t \tag{20}$$

Where $y_p(t)$ is *the particular solution*, and $G(\omega)$ is *the frequency response function*.

The shaker table obeys the rules of a linear time-invariant system and therefore, the transient and steady state solutions can be combined using the principle of linear superposition to obtain the overall system response. For this particular system, the transient solution is zero, and adding it to the particular solution does not change the solution. Therefore, this system is comprised of the steady-state response given by Equation (20).

The solution shown in Equation (20) describes the response of the simplified model, but it is still expressed in terms of generic values. To use this equation with the AFRL shaker table, the material properties of the system have to be used to calculate the modal parameters of stiffness, mass, and excitation amplitude. The value of these parameters were found by applying the previously mentioned assumptions, and using the dimensions of the shaker cross-section shown in Figure 13.

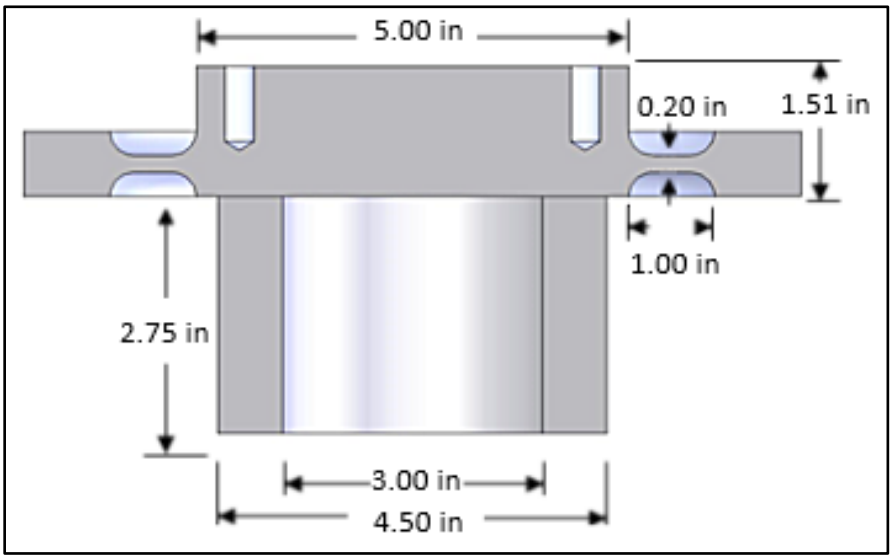

Figure 13. Two-Dimensional Shaker Table Model Dimensions

The shaker table material properties used to calculate the modal parameters of the simplified model are shown in Table 2.

Table 2. Published Material Properties of Shaker Table Components (Efunda, n.d.)

Material	**Shaker Component**	**Modulus of Elasticity (psi)**	**Density (lb/in^3)**
Titanium 64	Lid	1.65E+7	0.16
Copper 101	Piezo Stack	1.70E+7	0.32
PZT-5A	Peizo Stack	1.07E+7	0.28

For the AFRL shaker, the lid beam stiffness was calculated using the equation $k_b = \frac{12EI}{L^3}$. The beam was assumed to have a square cross-section with moment of inertia $I = bh^3/12$ and the stiffness was found to be $k_b = 2.74E+4$ lbf/in when using the dimensions shown in Figure 13.

The equivalent stiffness of the piezoelectric stack was calculated using a mechanics of materials relationship $k_{eq}=AE/L$, in which axial stiffness of a material is based on its cross sectional area, Modulus of Elasticity, and length. The piezoelectric was modeled as a stack of Copper (electrodes) and PZT-5A (piezoelectric) material connected in series having dimensions shown in Figure 13. Using the axial stiffness equation and considering the series connections, the equivalent piezoelectric spring stiffness was found to be $k_p = 2.06E+8$ lbf/in.

The value of the mass was calculated by multiplying the volume of the shaker lid test area, computed from the dimensions in Figure 13, and the density of titanium to obtain the value $M = 4.50$ lbs.

The excitation amplitude for the AFRL shaker table was calculated based on a property unique to the piezoelectric material. As described in the introduction, when the piezoelectric material has a voltage passed through it, the material deflects. The longitudinal expansion of the material is related to the voltage applied by a longitudinal deformation coefficient d_{33}. The axial expansion is magnified by increasing the number of piezoelectric crystals in the stack resulting in the excitation amplitude relationship $A = nd_{33}V$, where *A* is *excitation amplitude*, *n* is *number of piezo crystals*, d_{33} is *longitudinal deformation coefficient*, and *V*, is *applied voltage*. For the PZT-5A material used in this system, the deformation coefficient d_{33} has a value equal to 1.47E-8 in/V (Efunda, n.d.). The signal generator used to drive the AFRL piezoelectric shaker table produces a sinusoidal signal with 1400 volts maximum output. Using these values in the excitation amplitude relationship, the maximum amplitude of a four crystal stack was found to be A_{max} = 7.87E-5 in .

Calculation of the modal parameters was the last step to finalize the simplified model of the piezoelectric shaker table. Implementing the parameters calculated from the AFRL piezoelectric shaker table material properties into the steady state solution allowed the model to be used to determine the natural frequency and response of the system. The simplified 2D model response is given in the Preliminary Results section of Chapter IV.

Solid Model Construction

The creation of solid models for the piezoelectric shaker table components was a crucial first step to produce a finite element model. Most of the shaker components were relatively simple geometries easy to characterize with a few measurements, but to capture

the component details, they were scanned with an ATOS system to produce a three-dimensional point cloud. The ATOS scans of each component were completed with a 120mm measurement volume lens, and using a combination of 3mm and 0.8mm reference points. Full 360 degree scans were completed in 30 degree increments so twelve total scans were combined into a single 3D point cloud using reference point photogrammetry. Prior to exporting the data, the scans were processed to remove unwanted data from the surrounding support environment by highlighting the data and deleting the generated points.

The ATOS system software was used to export the component 3D point clouds in a Stereo Lithography (STL) file format that is compatible with most CAD suites. The STL files were then each imported into the SolidWorks 3D CAD software package as a mesh, shown in Figure 14, and the ScanTo3D surface wizard was used to convert the mesh to a 3D solid model. The wizard run used the guided surface creation option, and surface painting was completed using a combination of automatic and manual methods, as shown in Figure 14. Using SolidWorks surface functions, the painted surfaces were extracted, trimmed, knitted, and filled, as shown in Figure 14, to create the 3D solid component models. The ATOS scan data was completed in metric units, so the solid models were scaled by a factor of 25.4 to obtain a final solid model using English units. These models were checked for accuracy by measuring the geometries of the physical components with calipers and verifying the measurements in the solid models. All measurements were found to be within the 2.0E-3 inch margin of error reported for the ATOS scanner.

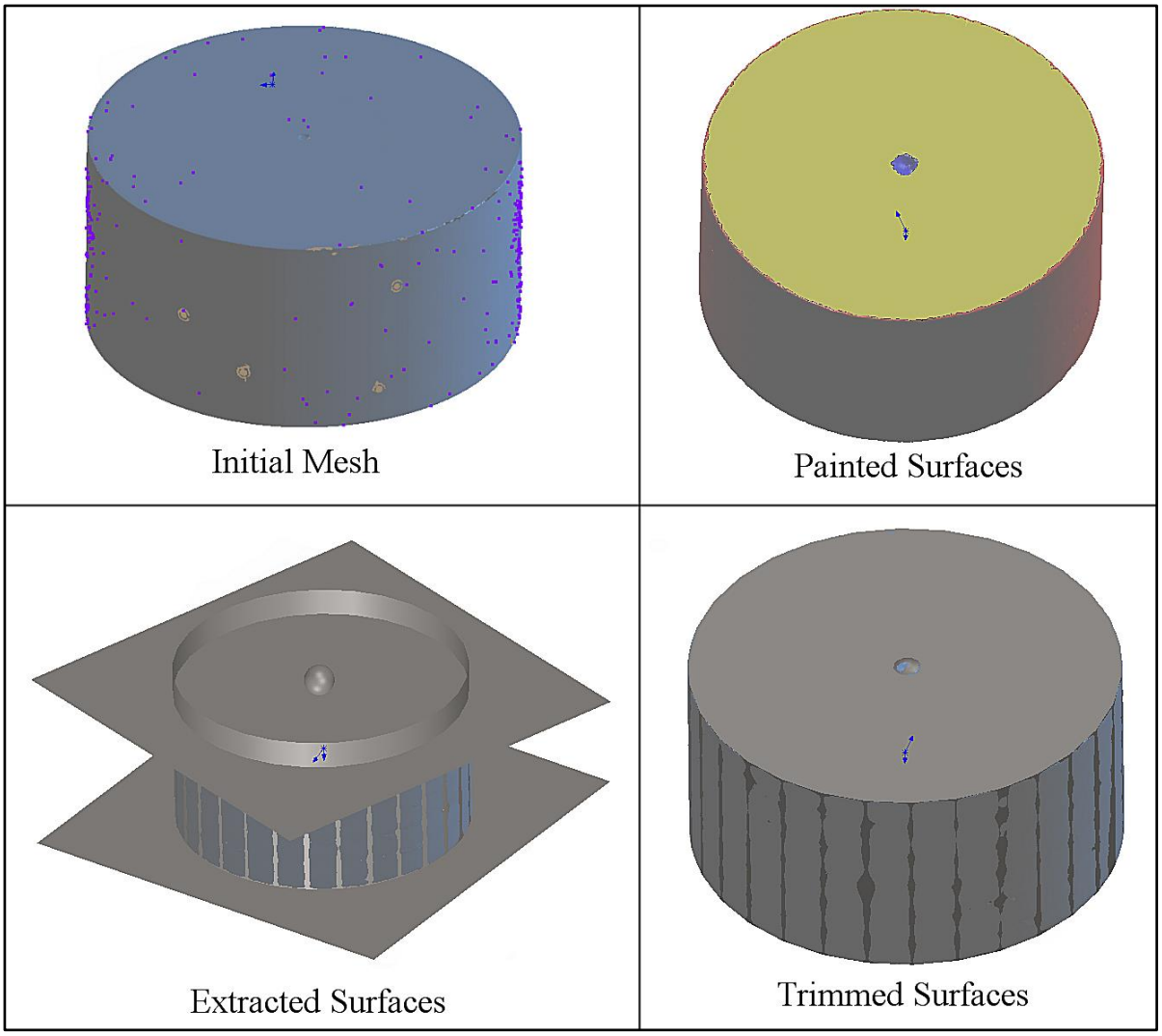

Figure 14. Spacer Component ScanTo3D Process

All of the shaker table components were scanned in this manner, but the thin flexible copper electrodes could not be captured accurately because when handled they changed shape enough to distort the scans. Therefore, the electrode solid model was created by measuring the geometry with a micrometer at several sampling points and using the mean value to produce the model in the SolidWorks 3D CAD software package. All measurements were accomplished using the same method. A representative

table of measurements highlighting the average electrode thickness is shown in Table 3.

Table 3. Electrode Solid Model Data

Electrode	Measurements			
	Thickness #1 (in)	***Thickness #2 (in)***	***Thickness #3 (in)***	***Thickness #4 (in)***
1	0.0099	0.0104	0.0102	0.0101
2	0.0103	0.0101	0.0097	0.0101
3	0.0098	0.0100	0.0103	0.0100
4	0.0104	0.0103	0.0100	0.0101
			Average Thickness	**0.0101**

The five piezoelectric crystals were scanned, but because of the crystals significance in the analysis, and the potential for surface contact issues in the finite element software package, the scans were not directly imported to create the crystal models. Instead, to generate a representative crystal to use in the FEM, the crystal scans were used to create an Initial Graphics Exchange Specification (IGES) file which contained the point cloud data. The IGES files were created by dividing the crystals into 45 sections along the Y-axis with one-tenth inch spacing between sections, as shown in Figure 15.

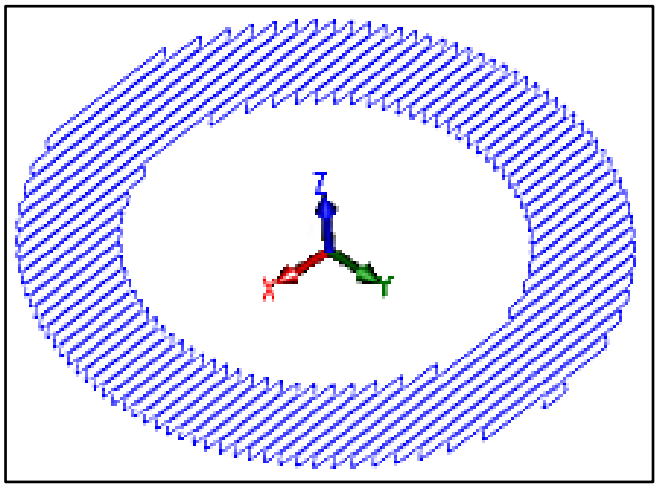

Figure 15. Piezoelectric Crystal Sections

IGES files are written in plain text, and the data was copied from these files into Microsoft Excel so each spreadsheet contained the X, Y, and Z coordinates of every point in the sectioned cloud. The data was sorted from smallest to largest value based on the value of the Z-coordinate. Once sorted, the coordinates of the crystal edges were removed so only the point cloud data of the top and bottom surfaces remained. Each spreadsheet contained approximately 60,000 data points for the surfaces, and these values were used to calculate the mean Z-coordinates and standard deviations shown in Table 4.

Table 4. Piezoelectric Crystal Surface Coordinates

Crystal	**Bottom Surface**		**Top Surface**	
	Mean Z-coordinate (in)	***STD Dev (in)***	***Mean Z-coordinate (in)***	***STD Dev (in)***
1	-1.24E-01	1.65E-03	-4.92E-05	6.87E-04
2	4.38E-04	9.65E-04	1.26E-01	8.48E-04
3	-1.22E-01	1.61E-03	3.57E-04	1.11E-03
4	-1.23E-01	6.73E-04	5.34E-05	6.85E-04
5	-1.25E-01	1.20E-03	-2.48E-04	6.81E-04

A 50,000 iteration Monte Carlo simulation was then run on the data to determine a thickness value of the representative piezoelectric crystal. Each iteration of the Monte Carlo simulation used the mean Z-coordinate and standard deviation to randomly generate a representative coordinate, which was used to determine the thickness of each crystal. The simulation stored the value of the iterations and produced an average thickness value based on all 50,000 iterations. A record of the final iteration values used in the simulation is shown in Table 5. This table is a small representation of the 50,000 tables produced in the simulation. The table highlights the piezoelectric crystal thickness results used to create the representative solid model.

Table 5. Final Piezoelectric Crystal Monte Carlo Simulation Iteration

Monte Carlo Simulation (50,000 Iterations)			
Crystal	**Bottom Surface Z-Coordinate (in)**	**Top Surface Z-Coordinate (in)**	**Thickness (in)**
1	-1.269E-01	1.858E-04	0.127
2	1.466E-03	1.253E-01	0.124
3	-1.209E-01	1.297E-03	0.122
4	-1.232E-01	1.960E-04	0.123
5	-1.254E-01	-3.335E-05	0.125
		Simulation Min	0.121
		Simulation Max	0.127
		Simulation Average	**0.124**

Determining the piezoelectric crystal thickness and creating a representative solid model for the crystals was the last step to produce a solid model for all the shaker components. Figure 16 shows the completed solid model geometries of the shaker table components. Detailed dimensions of each component can be found in Appendix A: Piezoelectric Shaker Table Component Dimensions.

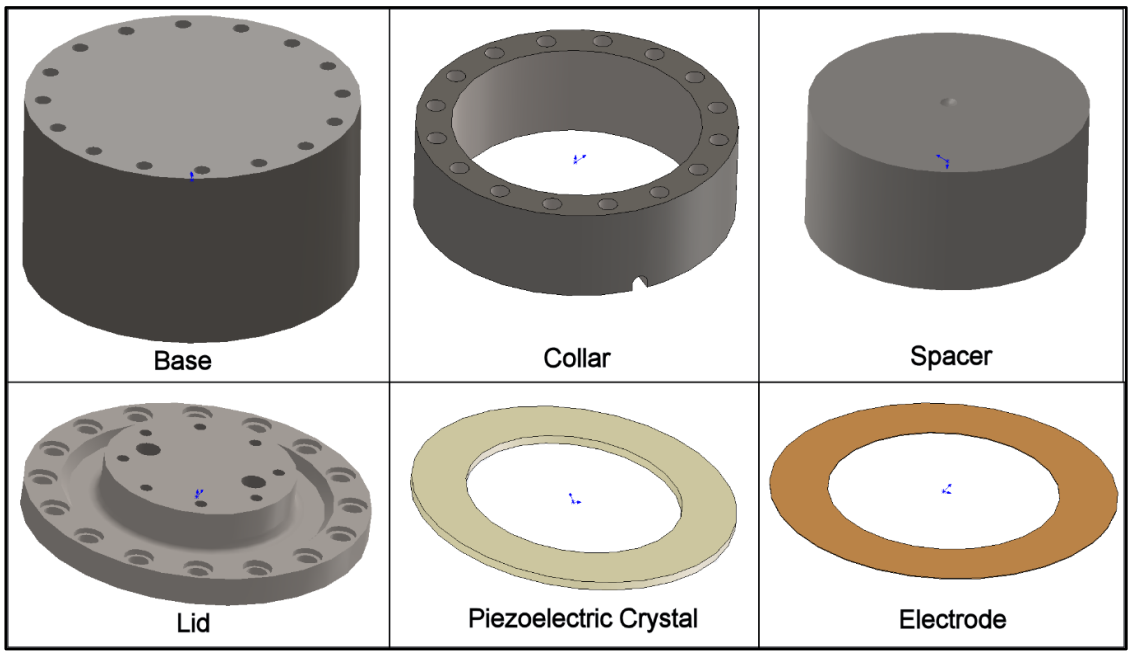

Figure 16. Piezoelectric Shaker Table Component Solid Models

Material Properties Evaluation

Finite element simulation accuracy is greatly affected by the material properties used in the analysis. For this reason, it was important to determine the exact material properties of the shaker table components used in the system FEM. However, because the components were already fabricated, and no raw materials were available, traditional destructive coupon testing methods were not possible. To find the exact material properties, an iterative process was adopted, but it required initial values as a starting point. The materials used to fabricate the AFRL piezoelectric shaker table components were specified by the manufacturer, and typical properties of the stated materials were located in a database to use as the starting point in the iterative process. The published results were not used as the exact values because variation in production methods result in variances around a mean value range for each property. Table 6 shows the initial material properties used for this approach.

Table 6. Initial Shaker Table Component Material Properties (Efunda, n.d.)

		Initial Values		
Component	**Material**	***Density (lb/in^3)***	***Young's Modulus (psi)***	***Poisson's Ratio***
Base Collar Spacer	Steel	0.284	2.90E+07	0.290
Lid	Titanium 64	0.160	1.65E+07	0.342
Piezo Crystal	PZT-5A	0.280	1.07E+07	0.310
Electrode	Copper 101	0.320	1.70E+07	0.320

The exact material properties were determined using a three step iterative process. First, finite element models with typical material properties were created for each of the shaker table components and a modal analysis was run. Next, a test where an impulse excitation force is generated by striking a component with a hammer, known as a ping

test, was conducted on the physical shaker table components to determine the actual modal response characteristics. Finally, the FEM modal response was compared to the experimental ping data, and the material properties were optimized until the modal results matched the ping data. Further details of the ping test and FEM process are outlined in the following sections.

Component Finite Element Simulations

To create component finite element simulations, the previously created solid models were exported in a file format compatible with the ANSYS Workbench FEA software package. The solid models were exported from SolidWorks in a highly portable Parasolid (x_t) file format, which could be imported into the ANSYS DesignModeler as an external geometry file. Once imported, the needed geometry was generated using DesignModeler functions. Linear elastic isotropic properties of density, Young's Modulus, and Poisson's Ratio were entered as ANSYS Workbench engineering data to define materials used in the finite element simulation. The properties entered into the ANSYS engineering data table were the initial values previously shown in Table 6.

After importing the geometry and specifying material properties, ANSYS Workbench modal analysis was chosen, and the ANSYS Mechanical module was run to prepare the finite element simulation. In this module, the material properties were assigned to imported geometries before generating a finite element mesh. Several mesh sizes were then created by specifying geometry face sizing to study convergence using a 3D 10-Node tetrahedral structural solid element (SOLID187). This element, shown in Figure 17, was chosen over both an 8-Node and 20-Node 3D structural solid because it

was described in the ANSYS documentation as being well suited for irregular meshes typically required of imported CAD geometries (ANSYS, 2014).

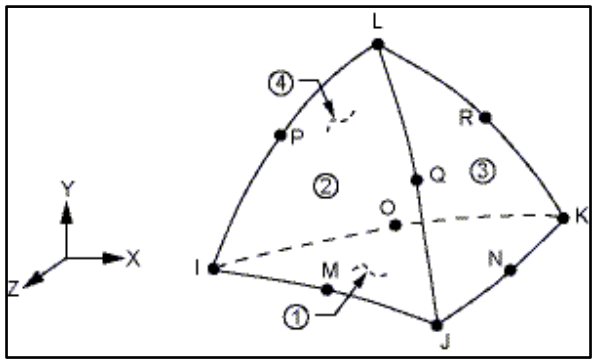

Figure 17. 3D 10-Node Tetrahedral Structural Solid Element (SOLID187) (ANSYS, 2014)

To run the finite element simulation analysis, settings were programmed to find all modes between 0 and 20,000 Hz using a direct solver. No boundary conditions were specified to ensure the modal solution captured the results of a free-free system. This process was accomplished for all the shaker table components. The specific mesh type, mesh sizing, and number of elements run which caused frequency to reach a steady state in the convergence study of each component is shown in Table 7. The highlighted values in Table 7 represent the mesh quantities used to carry out the steps in subsequent sections of this chapter. A full discussion of the convergence results will be covered in the Chapter IV.

Table 7. Piezoelectric Table Component Finite Element Meshes

Component	**Element Type**	**Mesh 1 Elements**		**Mesh 2 Elements**		**Mesh 3 Elements**		**Mesh 4 Elements**	
		Size (in)	***No.***	***Size (in)***	***No.***	***Size (in)***	***No.***	***Size (in)***	***No.***
Base	SOLID187	2.00	5514	1.00	6247	**0.50**	8508	0.25	26841
Collar	SOLID187	2.00	4541	1.00	4886	**0.50**	5537	0.25	16016
Spacer	SOLID187	2.00	329	1.00	440	**0.50**	1361	0.25	5879
Lid	SOLID187	1.00	6266	0.50	8798	**0.25**	17971	0.18	36240
Piezo Crystal	SOLID187	0.75	20	0.50	53	**0.25**	147	0.10	1020
Electrode	SOLID187	0.75	24	0.50	54	**0.25**	145	0.10	1029

The component geometries meshed using the converged face sizing specified in Table 7 are shown in Figure 18. Creation of these geometries with a converged mesh was the final step to complete the component finite element model simulations.

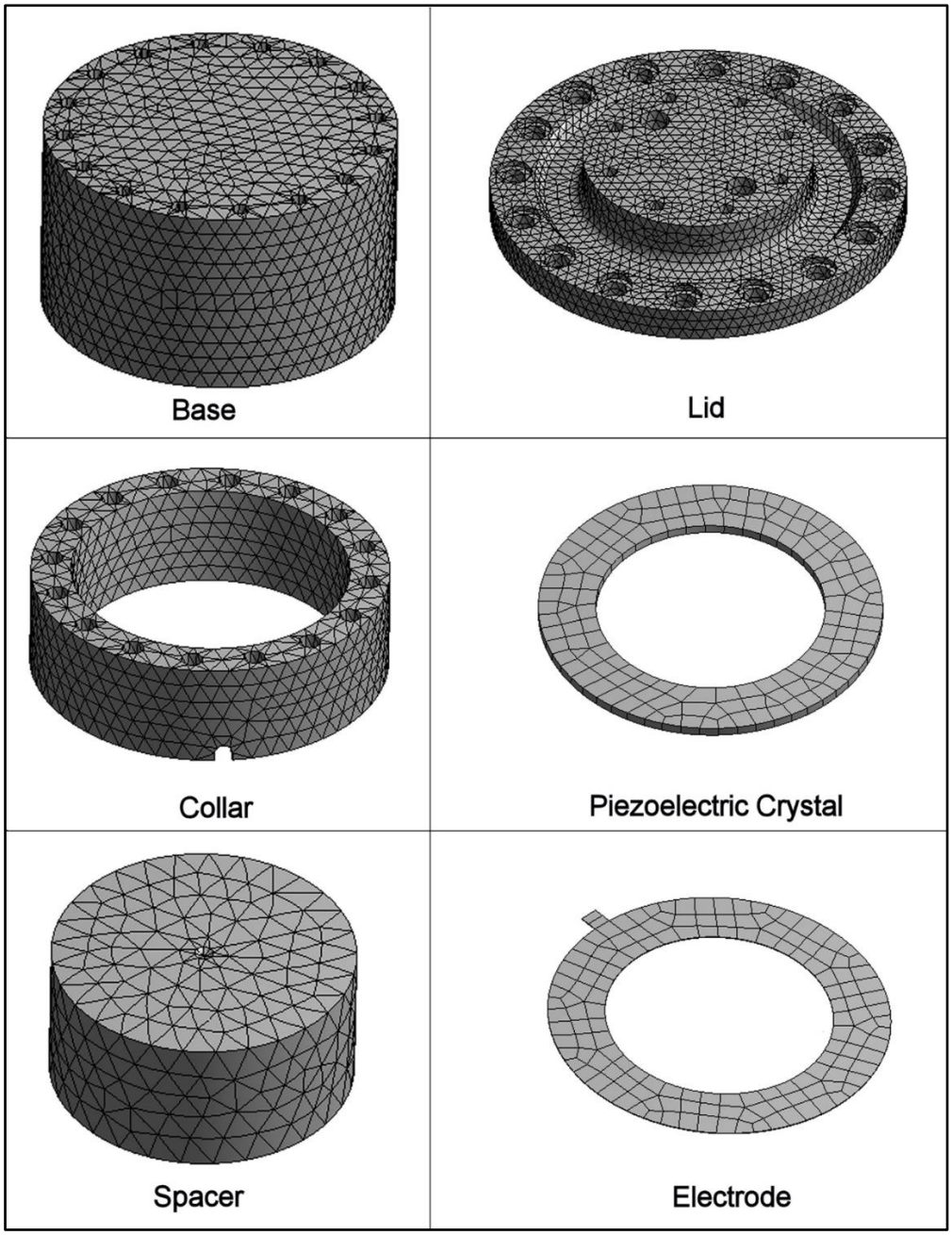

Figure 18. Piezoelectric Shaker Table Component Meshes

Component Ping Testing

Ping tests were conducted to determine the actual modal response characteristics of the piezoelectric shaker table components. The test data was collected to provide a basis for tuning the finite element modal response so the component material properties could be determined. For the ping tests to be a viable basis for finite element tuning, the test environment had to simulate a free-free support system. A Fabreeka FABCEL 25 vibration isolating neoprene pad was used as a support during the ping tests to produce the needed free-free conditions.

To confirm the FABCEL 25 support produced free-free conditions, the finite element simulations were run again with an elastic support foundation. The elastic foundation stiffness used in the simulations was determined from the FABCEL data sheet provided by the manufacturer. This data sheet included a load deflection curve, shown in Figure 19, which contained the data needed to determine the foundation stiffness.

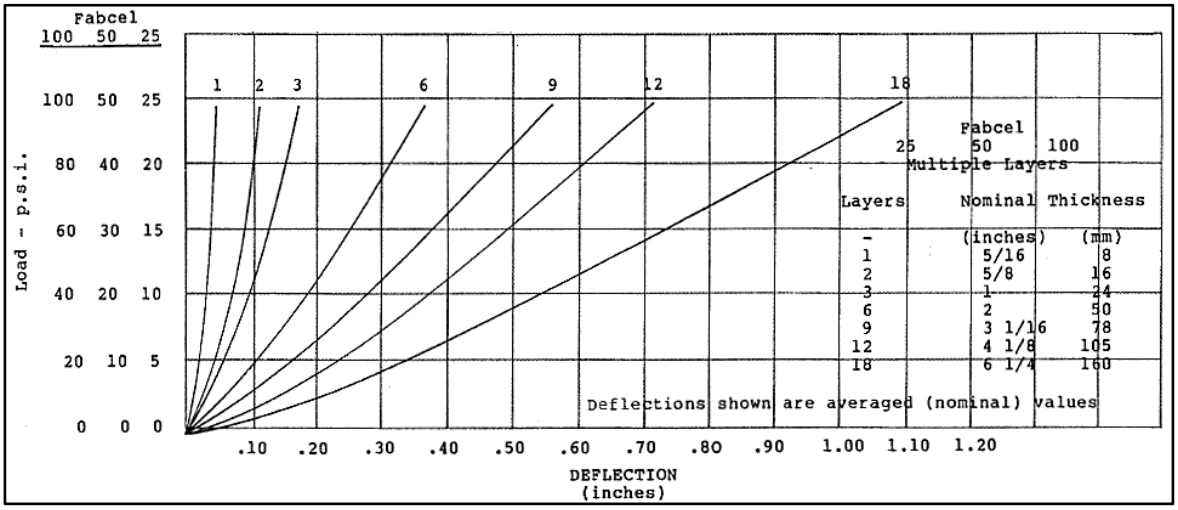

Figure 19. FABCEL 25 Load-Deflection Curve (FABCEL, 1994:3)

The maximum load applied to the FABCEL pad by the components was less than five pounds per square inch, as shown in Table 8, which fell in the region of the load-deflection curve, which could be approximated as a linear relationship. Data points were extracted from Figure 19 using the open source software Data Thief, which was created to capture curve data from images. From this data, a linear curve representing the elastic support foundation stiffness was created, shown in Figure 20 below. The mined data used to generate the curve can be found in Appendix B: Extracted FABCEL 25 Data Sheet Information.

Table 8. Component Loads Applied to FABCEL Isolator

Component	**Contact Area (in^2)**	**Weight (lbs)**	**Load (psi)**
Base	63.62	89.30	1.40
Collar	25.13	16.20	0.64
Spacer	16.05	10.00	0.62
Lid	25.13	7.90	0.31
Crystal	8.84	0.30	0.03
Electrode	8.84	0.03	0.00

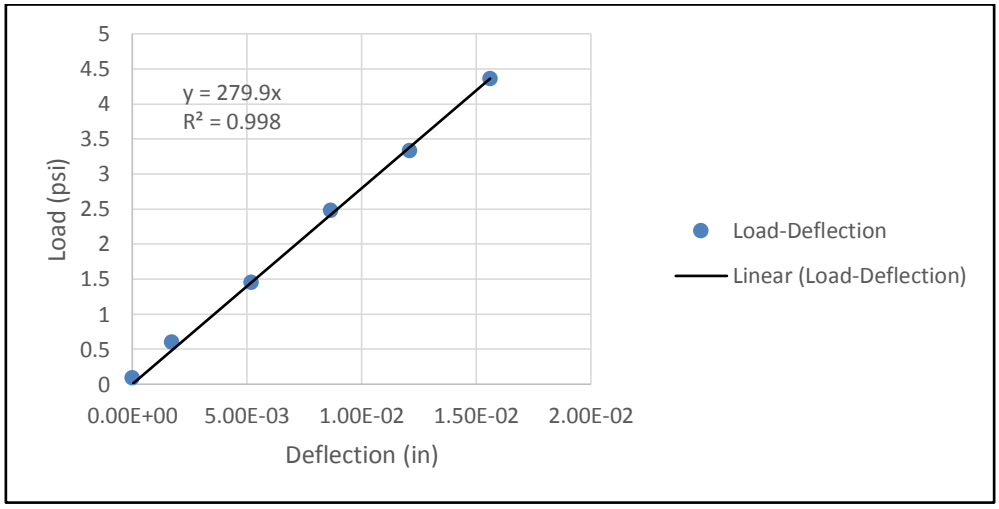

Figure 20. FABCEL 25 Linear Load-Deflection Approximation

The extracted value of 279.9 lbf/in^3 for linear elastic foundation stiffness was entered into the component finite element as an elastic support. The finite element simulation results, shown in Table 9, indicate the FABCEL 25 isolation pads provided free-free conditions for the base, collar, spacer, and lid components, but did not provide the same conditions for the crystal and electrode. At this point the possibility of tuning the piezoelectric crystal and electrode finite element models was abandoned, and published data was used for their material properties in all remaining work.

Table 9. Effects of Elastic Support on Component Finite Element Simulation

Component	Free-Free 1st Mode (Hz)	Elastic Support 1st Mode (Hz)	Percent Difference
Base	7273.70	7273.80	0.0014%
Collar	1473.00	1473.00	0.0000%
Spacer	13510.00	13510.00	0.0000%
Lid	1739.80	1745.90	0.3494%
Crystal	527.53	282.20	86.9348%
Electrode	48.80	909.39	94.6338%

After verifying that the FABCEL isolation pad provided free-free conditions, ping test data collection continued for the base, collar, spacer, and lid. The piezoelectric shaker table components were tested using the experimental setup shown in Figure 21. The test equipment included a Polytec PDV 100 single point laser vibrometer, ping hammer with nylon impact tip, National Instruments analog-to-digital conversion box, and a laptop computer.

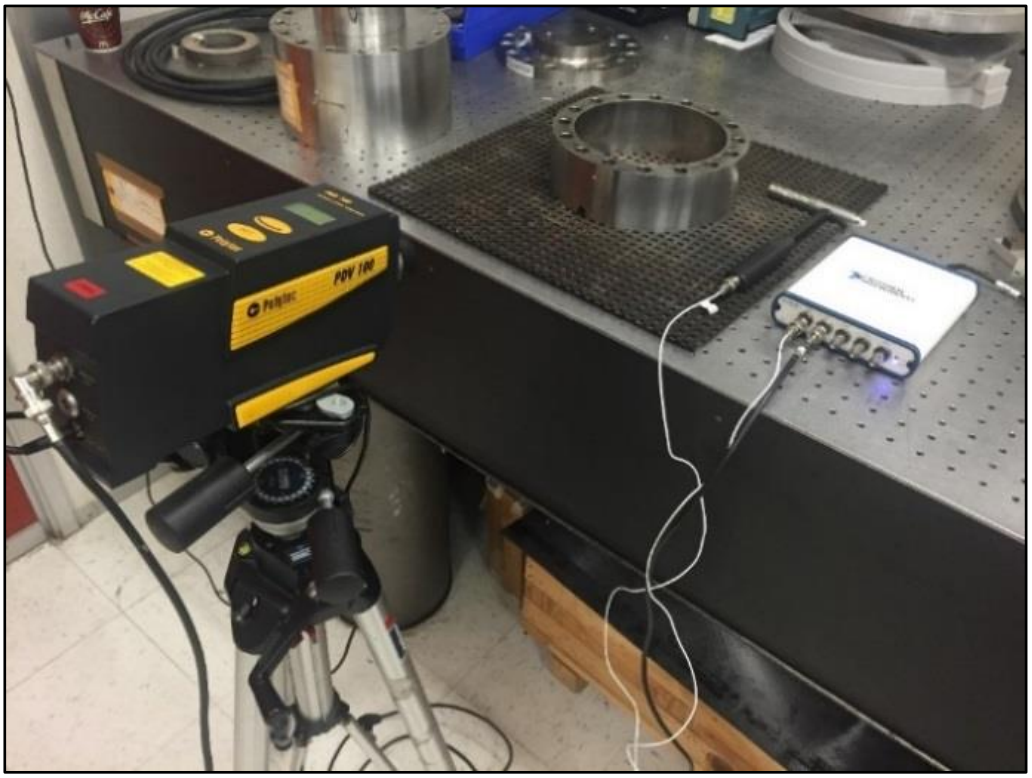

Figure 21. Ping Test Experimental Setup

The Polytec vibrometer settings were configured so the device reported velocity to the laptop computer at a ratio of 125 mm/s per volt. This setting is based on the one volt maximum output of the laser, but output is actually in millivolts, and configuring the laser to this level set the fidelity of the measurements at 5E-03 in/s per millivolt with a maximum velocity of 5 in/s. The laptop software used was a National Instruments LabView program created by AFRL, and it was configured to trigger data recording when the ping hammer applied a minimum of a 100 pound trigger force to the test article. The LabView software collected velocity data from the laser in the time domain and converted the data to the frequency domain by applying a fast Fourier transform. The laser was positioned to take measurements from the top surface of the components, and

they were pinged in multiple locations, as shown in Figure 22, to obtain several data sets. The base, spacer, and collar were all pinged and measured in the same locations shown in the representation of the base in Figure 22.

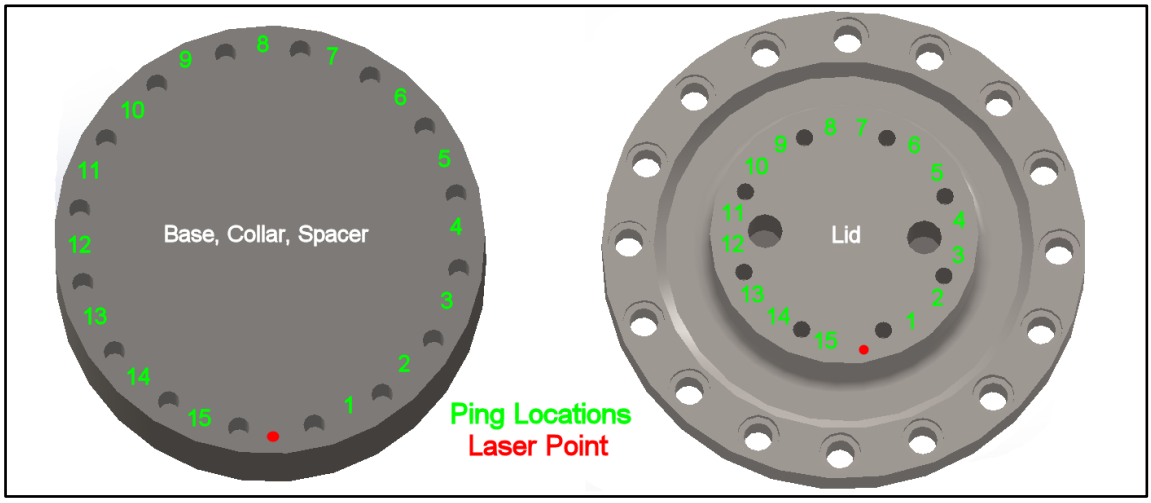

Figure 22. Component Ping and Laser Measurement Locations

Collection of test data for the base, collar, spacer, and lid components was the final step to component ping testing. The collected data was used in the finite element model tuning procedures to obtain the actual material properties of the components.

Component Finite Element Simulation Tuning

The finite element models for the shaker table components were created using linear elastic isotropic materials in which the properties are independent of direction. To define these materials in ANSYS Workbench the density, Young's Modulus, and Poisson's Ratio had to be entered. The process of tuning the finite element models required two of these three material properties be fixed while the third property was optimized until it forced the modal response to match experimental data. Density was

selected as the first material property to fix because it could be determined experimentally and input as a constant value.

To measure density, the weight and volume of the components had to be determined. The base, collar, spacer, and lid components were weighed using an Ohaus ES100L digital scale. The volume of the components was determined using the solid models created from the ATOS scans. The SolidWorks mass properties tool was used on each component to obtain volume values from the solid model geometries. The weight of each component was divided by the volume to find the component densities. The measured weights, volumes, and calculated densities are shown in Table 10 along with the typical published density values. Table 10 shows all of the calculated density values were within 3% of the typical published values. The measured density values were input into the finite element models to fix the density property. The steel components were not made from the same stock material, and therefore their density values shown in Table 10 are not identical.

Table 10. Measured Piezoelectric Shaker Table Component Densities (Efunda, n.d.)

Component	**Material**	**Weight (lbs)**	**Volume (in^3)**	**Measured Density (lb/in^3)**	**Published Density (lb/in^3)**	**Percent Difference**
Base	Steel	89.30	313.29	**0.285**	0.284	0.36%
Collar	Steel	16.20	57.50	**0.282**	0.284	0.80%
Spacer	Steel	10.00	34.78	**0.288**	0.284	1.22%
Lid	Ti-6-4	7.90	50.78	**0.156**	0.160	2.85%
Crystal	PZT-5A	0.30	1.10	**0.273**	0.280	2.67%
Electrode	Copper	0.03	0.09	**0.333**	0.320	4.00%

The second property fixed in the finite element models was Poisson's ratio. Although no tests were conducted to determine Poisson's ratio, the published data for this

property was relatively consistent between multiple sources. Additionally, small variations in Poisson's ratio had little to no effect when implemented in the finite element models so it was fixed at the typical values shown in Table 6.

After fixing density and Poisson's ratio in the finite element models, Young's modulus was optimized until the finite element modal solution for the first natural frequency matched the average value of the fifteen ping test experimental results. The iterative optimization process for tuning component natural frequencies began with data from Table 6, and the values were adjusted based on the difference in natural frequency between the finite element model and ping data. This process was completed when the first natural mode of the model matched ping test data. The modulus at this final point was the value used in the system finite element model to represent the true modulus of elasticity of the component. The full results obtained from this procedure will be further discussed in Chapter IV.

System Finite Element Simulation

The overall goal of this research was to produce a validated finite element model of the full system and not just the individual components. However, determination of the material properties was a critical step to fully characterize the individual component properties used in the full system assembly. The system finite element model quickly followed the component models because it was simple to produce an assembly of the already characterized components.

To generate a system model, the individual solid models were opened in SolidWorks and assembled using the mate feature to specify relationships between the

component geometries. The final system solid model assembly imported into ANSYS Workbench is shown in Figure 23. The actual piezoelectric shaker table assembly is also shown in Figure 23 for comparison to the completed solid model.

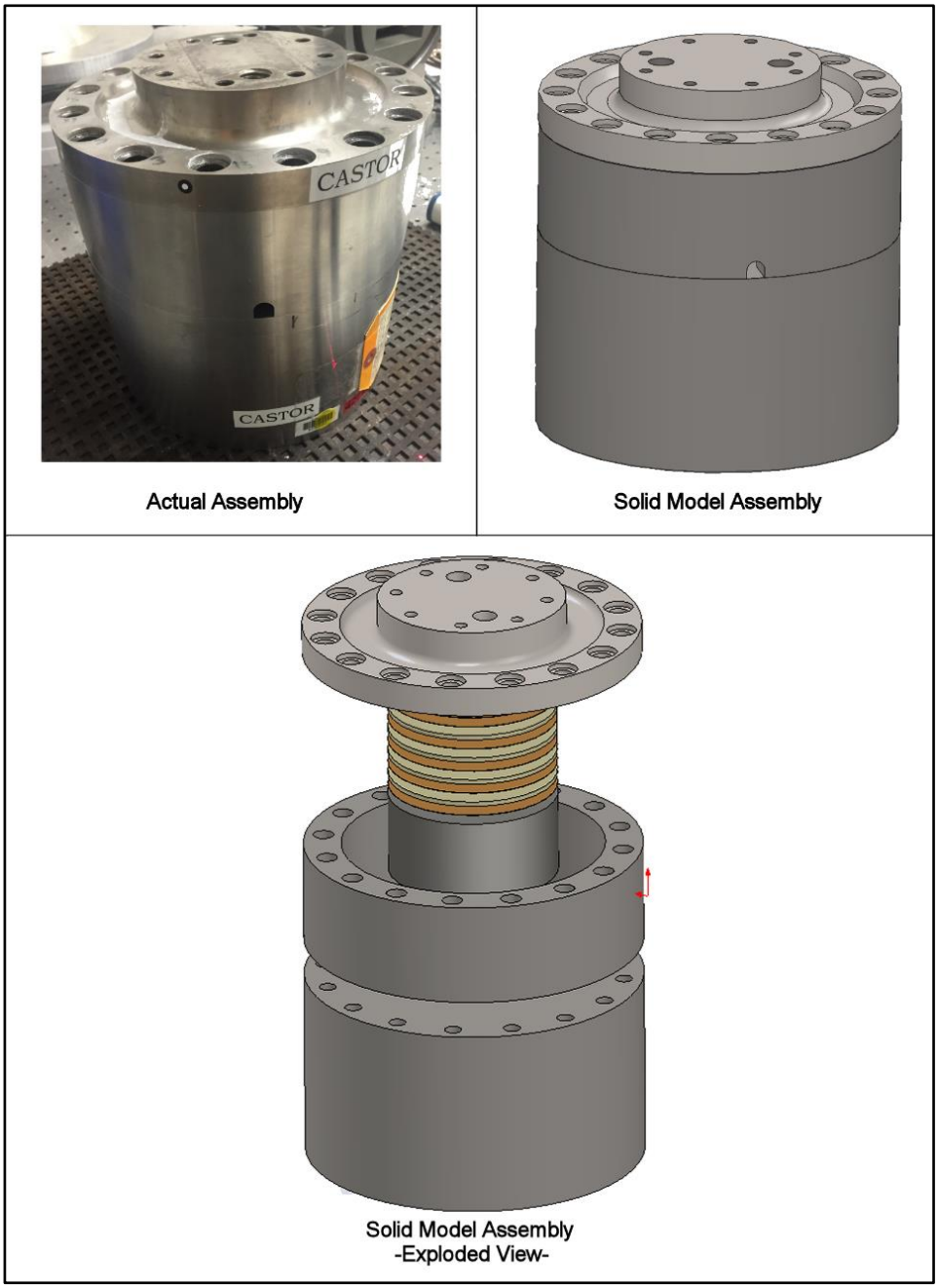

Figure 23. Piezoelectric Shaker Table System Solid Model

The system solid model geometry was imported into ANSYS using a Parasolid file and the same procedure followed for the individual components. After importing the geometry, updated material properties from the tuning process were specified in engineering data tables, and a harmonic response was added to the modal analysis so the frequency response could be captured graphically. ANSYS Workbench Mechanical was run to prepare the finite element modal and harmonic simulations.

In the ANSYS Mechanical module, steel, copper, titanium, and piezoelectric material properties were assigned to imported geometries for the modal analysis. Contact regions were used to specify connections between the components. Bonded connections were assigned to any components that were in contact with each other. The connections were specified as a Multi Point Constraint (MPC) formulation to ensure rigid connections between the component elements. This formulation was used because the 100 ft-lb torque of the tightened bolts produced an approximate 12,000 lb force that caused the components to remain rigidly connected.

The model was prepared for a mesh by specifying geometry contact and face sizing, and several meshes were generated to study convergence of the finite element solution. The meshes were generated using the 3D 10-Node tetrahedral structural solid element (SOLID187) previously shown in Figure 17. This element was chosen earlier for the component mesh because of its suitability for irregular meshes typical of complex CAD geometries, and it was once again selected for the system finite element model. The specific mesh type, element sizing, and number of elements run for convergence is shown in Table 11.

The highlighted values in Table 11 represent the converged mesh quantities that were used in the final system model and the meshed geometry is shown in Figure 24. A full discussion of the convergence results will be covered in the Chapter IV.

Table 11. System Finite Element Mesh Specifications

Component	Element Type	Mesh 1 Elements		Mesh 2 Elements		Mesh 3 Elements		Mesh 4 Elements	
		Size (in)	*No.*	*Size (in)*	*No.*	*Size (in)*	*No.*	*Size (in)*	*No.*
Base	SOLID187	3.00		2.00		**1.00**		0.50	
Collar	SOLID187	3.00		2.00		**1.00**		0.50	
Spacer	SOLID187	3.00	10935	2.00	14003	**1.00**	18358	0.50	34870
Lid	SOLID187	1.00		0.75		**0.50**		0.25	
Piezo Crystal	SOLID187	1.00		0.75		**0.50**		0.25	
Electrode	SOLID187	1.00		0.75		**0.50**		0.25	

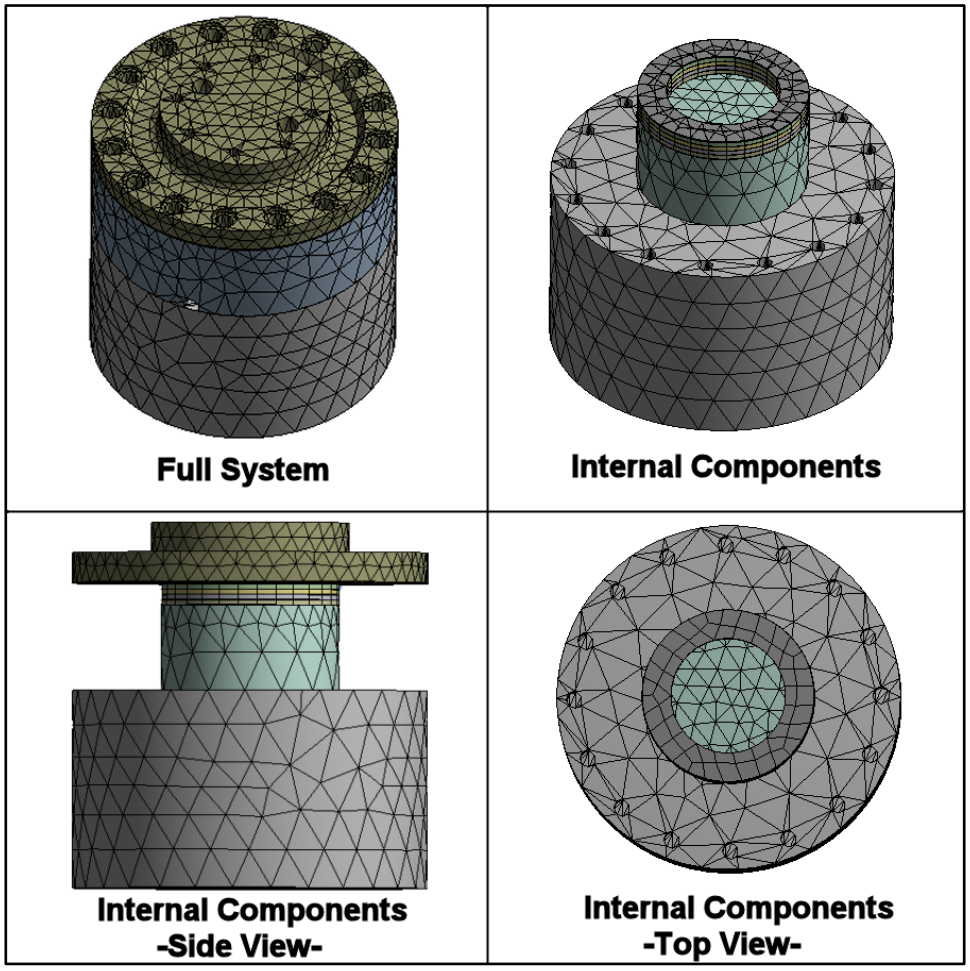

Figure 24. System Finite Element Mesh

To run the finite element modal analysis, ANSYS settings were configured for a direct solver that would find all modes in the piezoelectric shaker tables operating range of 0 to 50,000 Hz. A displacement support was placed on the bottom surface of the base component, which constrained the axial displacement of that face to zero. This support simulated the effects of the piezoelectric shaker table resting on the table. Configuring this support was the final preparatory step, and the finite element simulation was run for each of the convergence study mesh sizes. A full discussion of the convergence results will be covered in the Chapter IV.

After completing a modal analysis, the ANSYS Workbench Mechanical module was used to construct the harmonic response of the system. The harmonic analysis was configured to generate a frequency response plot of the system between 0 and 50,000 Hz. The number of solution intervals was set to 250 for this analysis to produce 25 Hz iterations (50,000 Hz / 250 intervals = 25 Hz / interval). A 500 lb sinusoidal force was applied to the shaker table lid to simulate the force applied by the piezoelectric crystals driven at 42 V. This force was an approximate value determined from the relationship between excitation amplitude and stiffness of the components, shown in Equation (21), which was derived in the simplified model.

$$F = Ak = nd_{33}V(2k_b + k_p) \tag{21}$$

The harmonic response analysis of the system was used to produce displacement and velocity frequency response functions exported to Microsoft Excel and will be further discussed in Chapter IV.

System Response Testing

As a final step, experimental tests were conducted to determine the modal response of the physical shaker table system. The purpose of these tests was to provide a basis of comparison for the finite element simulation. To begin system testing, the piezoelectric shaker table was completely assembled as shown in Figure 23. The shaker table system was connected to a signal generator, which supplied the piezoelectric crystals with a sinusoidal alternating current to excite a response. The crystal response provided a harmonic forcing function to drive the system through its range of operating frequencies. During the test, the physical response of the system was monitored using the experimental setup shown in Figure 25.

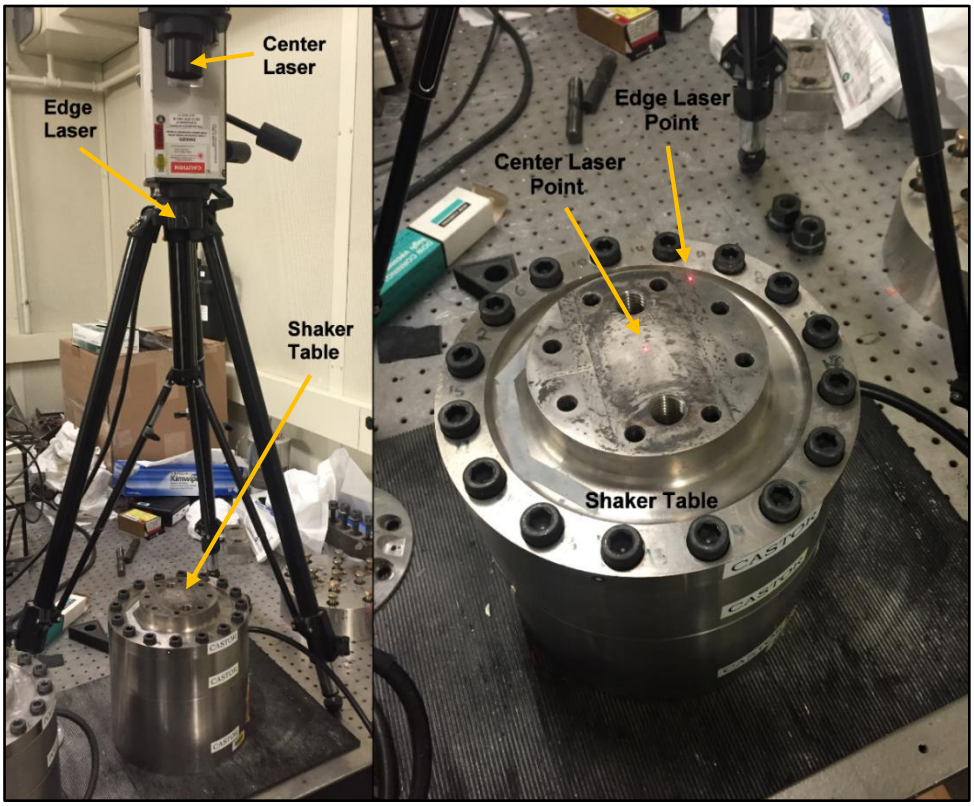

Figure 25. System Response Test Experimental Setup

The test equipment included two single point laser vibrometers, an Instruments Inc. Model S11-16 signal generator, Vibration Research Corporation VR9500 vibration controller, dell desktop computer, and VibrationVIEW software suite. The laser vibrometers were configured to measure displacement and velocity of center and edge points of the shaker lid, as shown in Figure 25. These positions were chosen because the finite element simulation predicted system modes that could not be captured by a single laser at the center of the shaker lid.

The VR9500 vibration controller was used in conjunction with VibrationView software to control the signal generator output and piezoelectric crystal excitation. The VibrationView software was programmed to make the signal generator sweep through a sinusoidal alternating current signal from 1,000 Hz to 50,000 Hz over a twenty minute test. This configuration resulted in 24.5 Hz frequency increments, which was consistent with the increments used in the finite element simulations. Three sweeps were run at steady 5 mV, 15 mV, and 30 mV input voltage levels to obtain multiple data sets over the typical AFRL range of operation. The signal generator produced a 1400 V gain and the corresponding output voltages applied to the piezoelectric crystals were 7 V, 21 V, and 42 V respectively. The collected data was exported from VibrationView in a Comma Separated Values (CSV) file format so it could be easily opened and processed in a spreadsheet.

The piezoelectric shaker table was disconnected from the signal generator after running the operational tests, and a ping test was conducted on the fully assembled system to obtain further data to validate the finite element model. The ping tests

performed on the full system assembly were conducted using exactly the same method and equipment outlined for the component ping tests.

Exporting VibrationView data and collecting fully assembled ping data were the final steps to complete system response testing. The collected data was used as a basis of comparison for the finite element simulation. The results of this comparison and all of the system response testing data will be further discussed in Chapter IV.

Summary

The procedures outlined in this chapter were logical steps taken toward the final thesis objective of producing a validated piezoelectric shaker table FEM. The approach used to achieve this goal was a combination of analysis and experimentation. The system was first characterized by an initial simplified model to gain understanding of system operation. Then individual shaker table component solid models and finite element simulations were created. These models were then compared to collected ping test data for the components in order to tune the material properties. With accurate material properties determined, the system solid model assembly and finite element simulation were then created. Experimental data was then collected for the physical system as a final step towards validating the model. All of the analysis and collected data was then compiled and processed in Microsoft Excel to produce the analysis and results discussed in Chapter IV.

IV. Analysis and Results

Chapter Overview

The purpose of this research was to create and validate a FEM for the AFRL piezoelectric shaker table. This goal was accomplished using the methodology outlined in Chapter III to accomplish several preliminary steps. These steps were taken to ensure the accuracy of the final product and each one produced results used to generate the system FEM.

The first of these steps, an initial simplified model, resulted in a natural frequency prediction and deeper understanding of the piezoelectric shaker table which was invaluable in creating the system FEM. Next, finite element and experimental test results were obtained, and an iterative process was used to compare them so the material properties of the system could be determined. The resulting component material properties were used in the full system FEM. Finally, frequency response results were obtained from the system FEM and experimental testing of the physical shaker table system.

Overall, the two main results obtained were the system finite element response and physical system response. The majority of discussion in this chapter will focus on these results. However, many of the steps taken produced intermediate results that were not directly compared to the final solution, but they were still important to achieve the system model and require discussion.

Preliminary Results

Simplified Model

The simplified model developed as a first step in this research was motivated by determining the system natural frequency. It was a one-dimensional SDOF representation of a complex continuous 3D system, and it resulted in a single natural frequency. However, the ease of calculating this solution, when compared to producing the finite element model, makes it an easy way to quickly determine at least one frequency of interest.

The natural frequency was calculated using model characteristics previously determined during the simplified model design. These values were substituted into Equation (22) to determine the simplified model natural frequency $\omega_n = 21{,}161$ Hz . At the time this value was calculated, it was the first available result, and the only reasonable evaluation of its legitimacy was to ensure it was in the operating range of the shaker table. Further evaluation of this result was conducted once the finite element model and physical table responses were obtained, and these results will be further discussed when the response data is presented.

$$\omega_n = \frac{1}{2\pi}\sqrt{\frac{k_{eq}}{m}} = \frac{1}{2\pi}\sqrt{\frac{12\,\frac{in}{ft}\left[2\left(k_b\,\frac{lb}{in}\right) + \left(k_p\,\frac{lb}{in}\right)\right]}{m\ lb\left(0.031081\,\frac{slug}{lb}\right)}} \tag{22}$$

As the model was developed, it also produced several meaningful results beyond the initial intent of determining the systems natural frequency. Using Equation (21) the

simplified model was also found to be a quick tool in determining the approximate displacement amplitude, applied force, and maximum voltage. Some of these unexpected results, such as the applied forcing function, were even implemented into the final system model as described in Chapter III.

Equations for determining the displacement amplitude and applied force were previously described Chapter III. However, the approximate maximum voltage V_{max} = 1124.3 V was determined using Equation (21) in combination with the yield strength of the piezoelectric crystals (~2900 psi), as shown in Equation (23). In this equation the 12,000 lb pre-load of the tightened bolts was calculated using the relationship F_{pre} = T/cD, where T was the 100 ft lb torque of the bolts, c was the constant 0.2 coefficient of friction for steel threads, and D was the 0.5 in bolt diameter.

$$V_{max} = \frac{\sigma_y A - F_{pre}}{n d_{33}(2k_b + k_p)} \tag{23}$$

This relationship was approximate because it applied the simplifying assumptions of the SDOF model, but the calculated value was a reasonable number and it was within the operating range of the signal generator. More investigation is required on the subject, but this equation is still useful as an initial quick calculation to avoid resonating and failing crystal stacks.

Material Properties

An important initial step in producing the system finite element model was to determine the actual material properties of the shaker table components. The process

used to accomplish this involved the iterative tuning of component finite element model material properties and a comparison of the resulting solutions to experimentally captured frequency response data. The data captured during this process, and presented in this section, was obtained using the specific procedures outlined in the methodology.

Before using the component finite element models, a convergence study was conducted to determine the mesh size for each component which caused frequency to reach a steady state. The specific meshes used for the component convergence studies are shown in Table 12, and a plot of the results is shown in Figure 26.

Table 12. Component Convergence Study Meshes

Base			
Mesh	***Mesh Size (in)***	***No. of Elements***	***Frequency (Hz)***
1	2.00	5514	7286.5
2	1.00	6247	7275.6
3	**0.50**	**8508**	**7273.7**
4	0.25	26841	7271

Lid			
Mesh	***Mesh Size (in)***	***No. of Elements***	***Frequency (Hz)***
1	1.00	6266	1821.5
2	0.50	8798	1781.3
3	**0.25**	**17971**	**1739.8**
4	0.18	36240	1724

Collar			
Mesh	***Mesh Size (in)***	***No. of Elements***	***Frequency (Hz)***
1	2.00	4541	1505.3
2	1.00	4886	1477.4
3	**0.50**	**5537**	**1473**
4	0.25	16016	1465.7

Crystal			
Mesh	***Mesh Size (in)***	***No. of Elements***	***Frequency (Hz)***
1	0.75	20	530.31
2	0.50	53	528.41
3	**0.25**	**147**	**527.53**
4	0.10	1020	527.42

Spacer			
Mesh	***Mesh Size (in)***	***No. of Elements***	***Frequency (Hz)***
1	2.00	329	13726
2	1.00	440	13569
3	**0.50**	**1361**	**13510**
4	0.25	5879	13499

Electrode			
Mesh	***Mesh Size (in)***	***No. of Elements***	***Frequency (Hz)***
1	0.75	24	48.77
2	0.50	54	52.62
3	**0.25**	**145**	**48.8**
4	0.10	1029	48.72

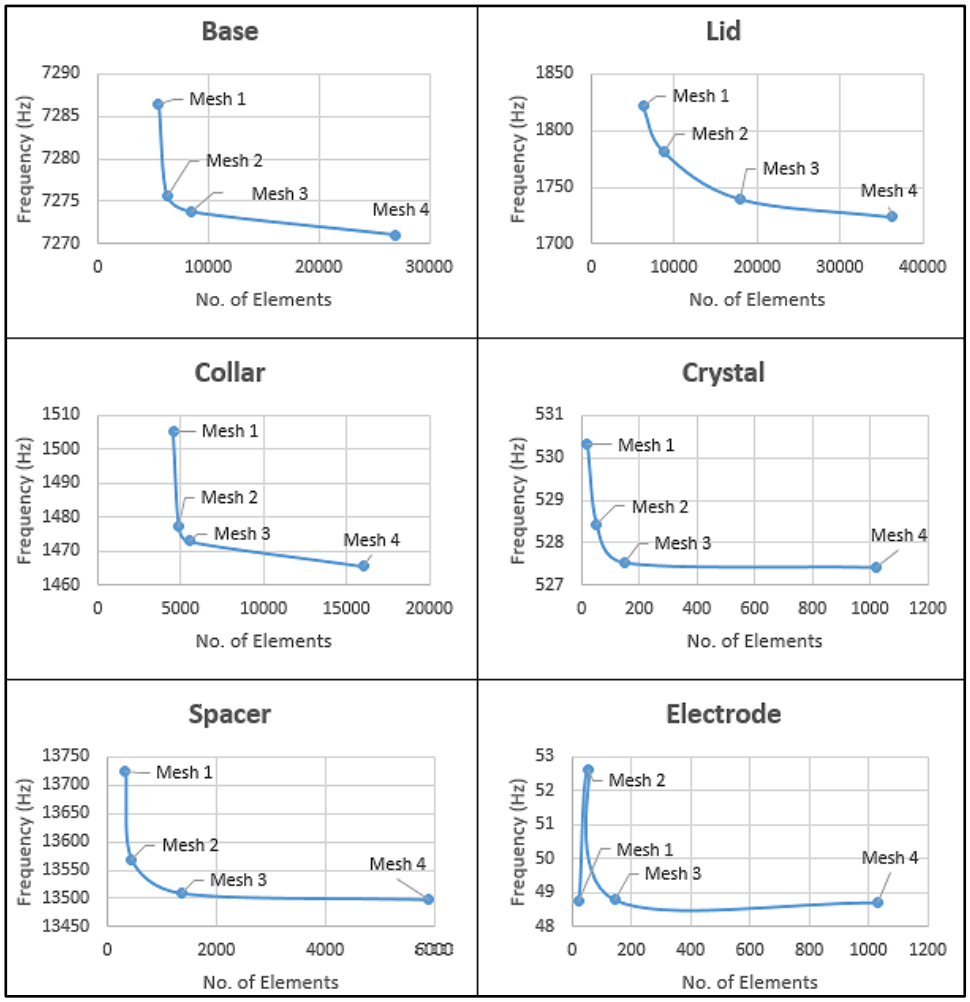

Figure 26. Component Convergence Results

The results of Figure 26 shows minimal improvement in accuracy of the solutions is acquired by increasing the mesh quality beyond the Mesh 3 sizing for each component. In fact, increasing the mesh quality beyond this level required three to five times more elements, and additional solution computation time to obtain a similar solution. Therefore, the component finite element solutions converged using Mesh 3 sizing indicated by the highlighted sections of Table 12. The results of this convergence study were then implemented in the finite element models and used in the iterative tuning process to determine component material properties.

The tuning process was completed by fixing density at the measured value for each component and Poisson's ratio at the published values, as shown in Table 13. As an initial starting point for the iterations, Young's modulus was also set to the published values shown in Table 13. However, the purpose of the tuning process was to determine a more accurate value for the modulus, and it was changed incrementally until the first natural mode of the component free-free FEM coincided with the first mode peak value from the ping test response data. Table 13 shows the resulting values of Young's modulus were then used in the system finite element model as true material properties of the components. The percent difference between the published initial values and the final tuned values, also shown in Table 13, emphasized the necessity of conducting the tuning process.

Table 13. Material Property Tuning Results

Component	**Material**	**Fixed Values**		**Untuned**	**Tuned**	**Percent Difference**
		Poisson's Ratio	***Density (lb/in^3)***	***Young's Modulus (psi)***	***Young's Modulus (psi)***	
Base	Steel	0.290	0.285	2.90E+07	**2.94E+07**	1.36%
Collar	Steel	0.290	0.282	2.90E+07	**2.82E+07**	2.83%
Spacer	Steel	0.290	0.288	2.90E+07	**2.92E+07**	0.68%
Lid	Titanium 6-4	0.342	0.156	1.65E+07	**1.55E+07**	6.45%
Crystal	PZT-5A	0.310	0.273	1.07E+07	**1.07E+07**	-
Electrode	Copper 101	0.320	0.333	1.70E+07	**1.70E+07**	-

Figure 27 provides a visual representation of how the natural frequency changed as Young's modulus was iterated in the tuning process. The complete set of ping data used to generate the plots in Figure 27 covered frequencies of 0 to 10,000 Hz for the base, collar, and lid components. The ping data for the spacer required a larger frequency range to capture the components first natural mode and it covered frequencies of 0 to

25,000 Hz. The plots of Figure 27 narrowed these data sets by limiting the range of the horizontal axes to more clearly visualize the tuning process.

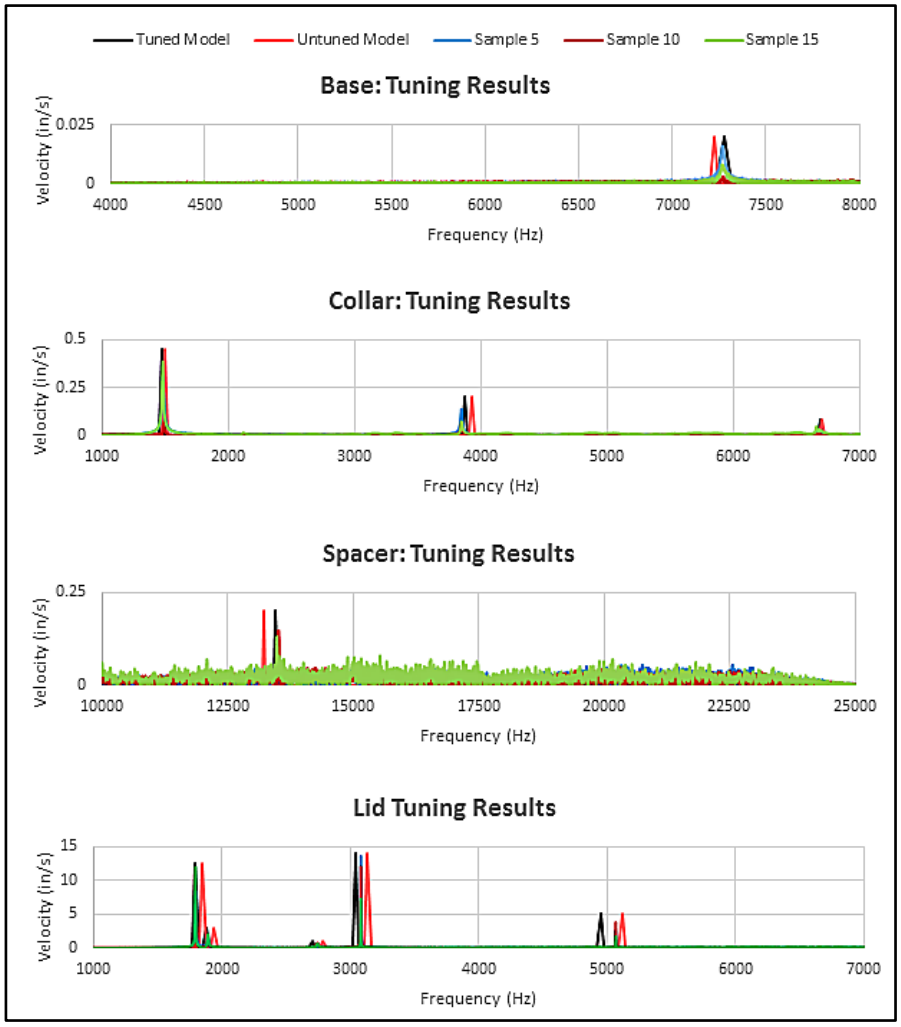

Figure 27. Component Frequency Tuning Results

Primary Results

The two main results obtained were the system finite element response and physical system response. These were considered the primary findings because they were the final results used to validate the total system finite element model created for this research.

To obtain the system finite element system response, the component finite element models were updated with material properties found during the tuning process. The component geometries were assembled, as previously shown in Figure 23, into a full system model. Before using this model for analysis, a convergence study was necessary to determine the mesh size which would capture converged results with the lowest element count. The stability of the 1st mode displacement solution, normalized by the ping data ratio of velocity to first natural frequency, was used as the convergence criteria. The specific meshes used for the convergence study are shown in Table 14, and a plot of the results is shown in Figure 28.

Table 14. System Convergence Study Meshes

Mesh	Mesh Size (in)						No. of Elements	Normalized 1st Mode Disp (in)
	Base	*Collar*	*Spacer*	*Lid*	*Crystal*	*Electrode*		
1	3.00	3.00	3.00	1.00	1.00	1.00	10935	1.71E-05
2	2.00	2.00	2.00	0.75	0.75	0.75	14003	1.51E-05
3	1.00	1.00	1.00	0.50	0.50	0.50	18358	1.48E-05
4	0.50	0.50	0.50	0.25	0.25	0.25	34870	1.45E-05

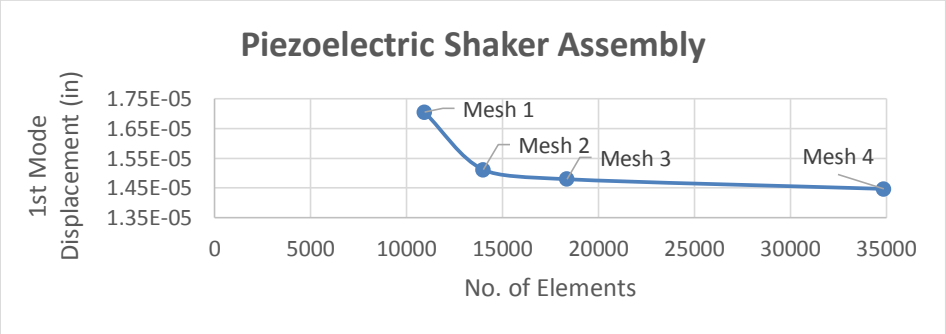

Figure 28. System Convergence Results

The results of Figure 28 show the solution converged at Mesh 3 sizing. As with the component convergence studies, this result indicated increasing quality beyond the

specified mesh size did not increase solution accuracy, but did require additional computational resources resulting in four to five hours of additional solve time. The converged Mesh 3 sizing is indicated by the highlighted sections of Table 14. The results of this convergence study were implemented in the final system finite element model, and the modal and harmonic analyses were run to obtain a FEA solution for system response.

The final step in obtaining the primary results for comparison and discussion was to analyze data obtained during the physical system response test. Multiple data sets were collected by varying the excitation voltage for each sweep of the shaker table operational frequency range. Three data sets were collected at 5 mV, 15 mV, and 30 mV input voltages, respectively, and the velocity and displacement results are shown in Figure 29 and Figure 30.

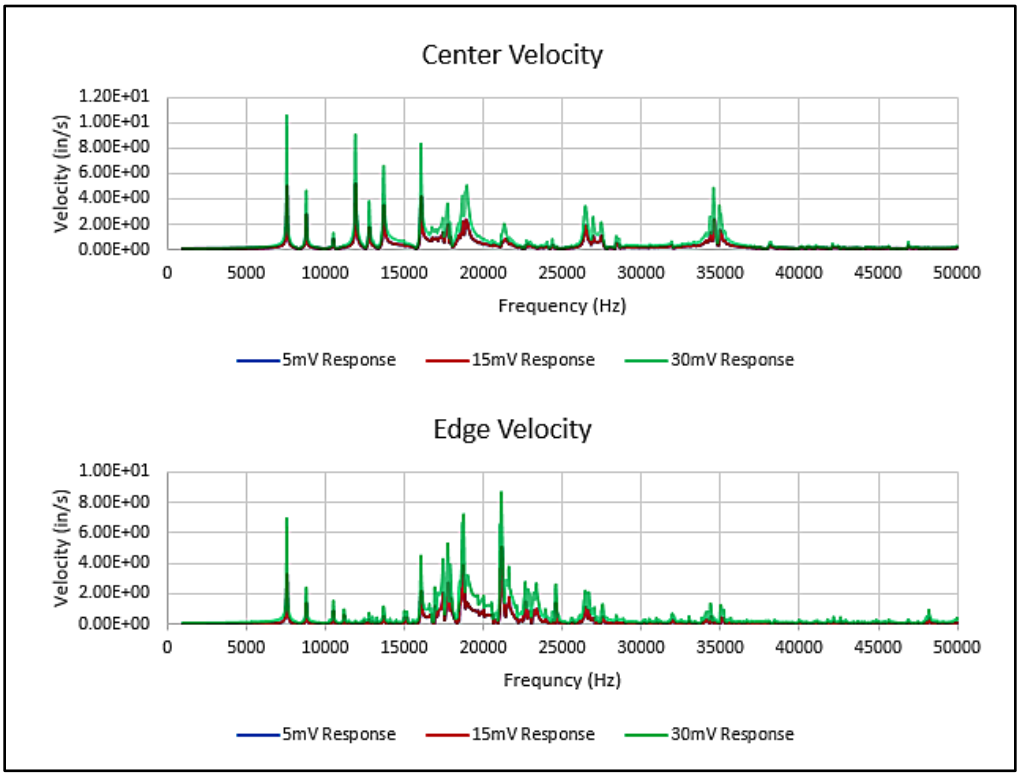

Figure 29. System Response Velocity Data Comparison

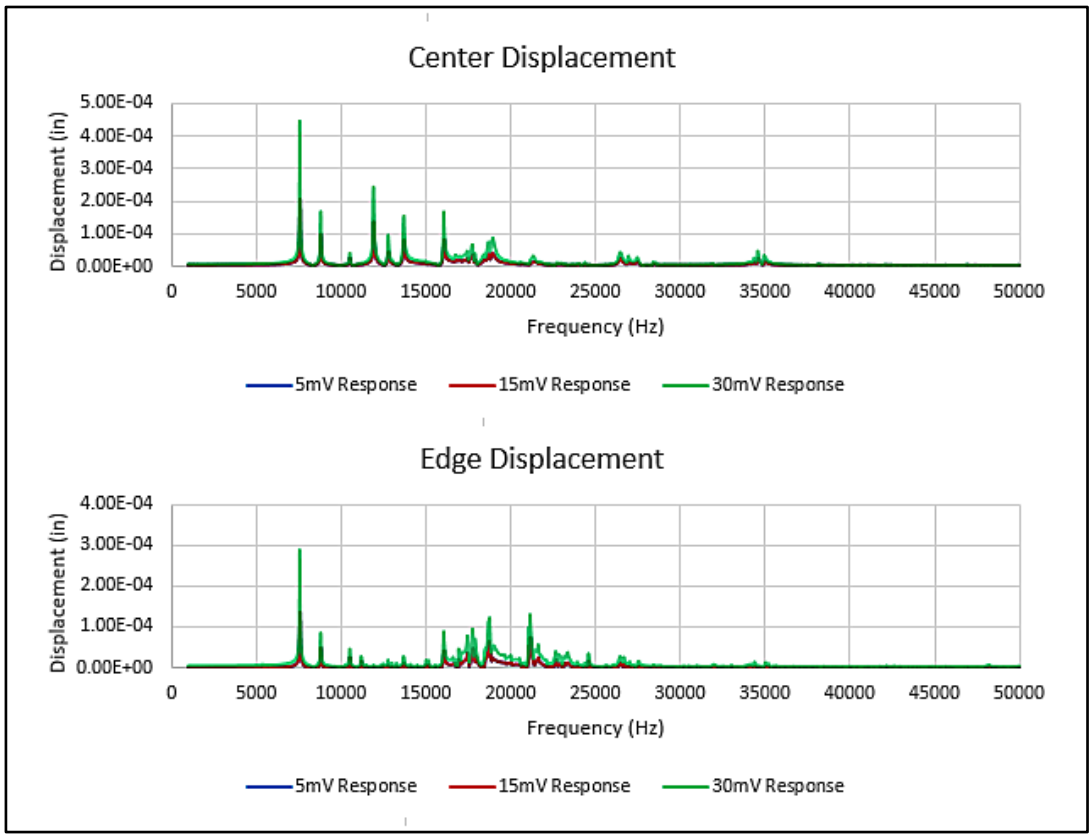

Figure 30. System Response Displacement Comparison

The data shown in Figure 29 and Figure 30 indicates only the amplitude of the natural frequencies change when the piezoelectric shaker table is operated at the specified voltage levels because the response is dependent on the mass (M) and stiffness (K) of the system and not the forcing function (F(t)). This result, which is based on the mathematical EOM, allowed the data to be narrowed to a single operating voltage for comparison with the finite element response data. An input voltage of 30 mV was used for the data set to compare with the finite element model because the simulation was run with a force calculated from the same voltage level in the simplified model relationships.

Determining an experimental data set to use for analysis allowed comparisons of the simplified model response, finite element model response, and system physical response to be generated. Two comparisons were made, the first was an evaluation of the free-free response of the finite element model and the free-free ping data obtained for the physical shaker table. The ping data was obtained without operating the crystals to decouple the electromechanical aspects as much as possible, so a purely mechanical response could be recorded. The normalized ping results for the system are shown in Figure 31, and a comparison of the extracted modal frequencies to the finite element results is shown in Table 15.

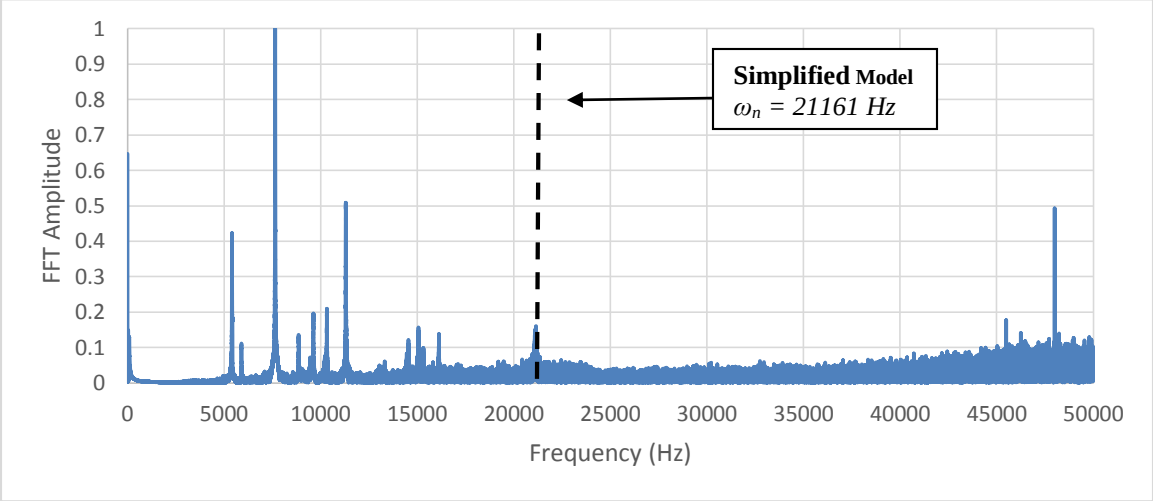

Figure 31. Piezoelectric Shaker Table Ping Test Response

Table 15. Comparison of Ping and FEA Free-Free Response (1st Five Modes)

Mode	Natural Frequencies		Percent Difference
	Ping Test (Hz)	*FEM (Hz)*	
1	5408	5812.6	7.48%
2	5896	5827.4	1.16%
3	7646	7930.1	3.72%
4	8857	9054.6	2.23%
5	9625	10297	6.98%

The ping results are a frequency response plot generated using the absolute value of a Fast Fourier Transform (FFT) performed on velocity data relative the static position. Each natural frequency peak has a corresponding phase angle that describes whether the velocity amplitude is in or out of phase with the initial impulse force generated when the component was struck by the ping hammer. The ping data captured the free-free response of the system to an impulse force, which supplied an initial velocity condition to the system. This response is governed by Equation (24), which is found by setting the forcing function to zero and characterizing the impulse force as an initial velocity ($\dot{y}$) in the solution to the differential Equation (25). The response is an exponentially decaying function that captures surface velocity data over time and a FFT algorithm is used to convert the data into the frequency domain shown in Figure 31.

$$g(t) = \frac{1}{M\omega_d} e^{-\zeta\omega_n t} \sin w_d t \qquad \text{for } t > 0 \tag{24}$$

$$M\ddot{y} + c\dot{y} + ky = 0 \tag{25}$$

Where *g(t)* is *impulse response*, *M* is *mass,* ω_d is *damped natural frequency*, ζ is *the viscous damping factor,* ω_n is *natural frequency*, and *t* is *time.*

The results shown in Table 15 indicate the mechanical response of the FEA roughly matches the systems physical response, and the finite element model predicts the natural frequency within 10% of experimental data, as can be seen in Table 15. Additionally, the natural frequency, ω_n = 21,161 Hz, predicted by the simplified model is within 0.11% of a natural frequency obtained from the ping data, as shown in Figure 31.

The mode shapes corresponding to the first five modes of the system are shown in Figure 32. As indicated in the ping data, the first two modes are close, and Figure 32 shows that they have a similar tilting mode shape in which the lid and collar tilt in the same direction. The third mode is also a tilting mode, but the collar has sliding motion rather than the tilting motion of the first two modes. The fourth and fifth modes are both rocking modes in which the lid rocks back and forth, but this is an isolated motion in the fifth mode, and coupled a rocking motion in the collar in the fifth mode, both shown in Figure 32.

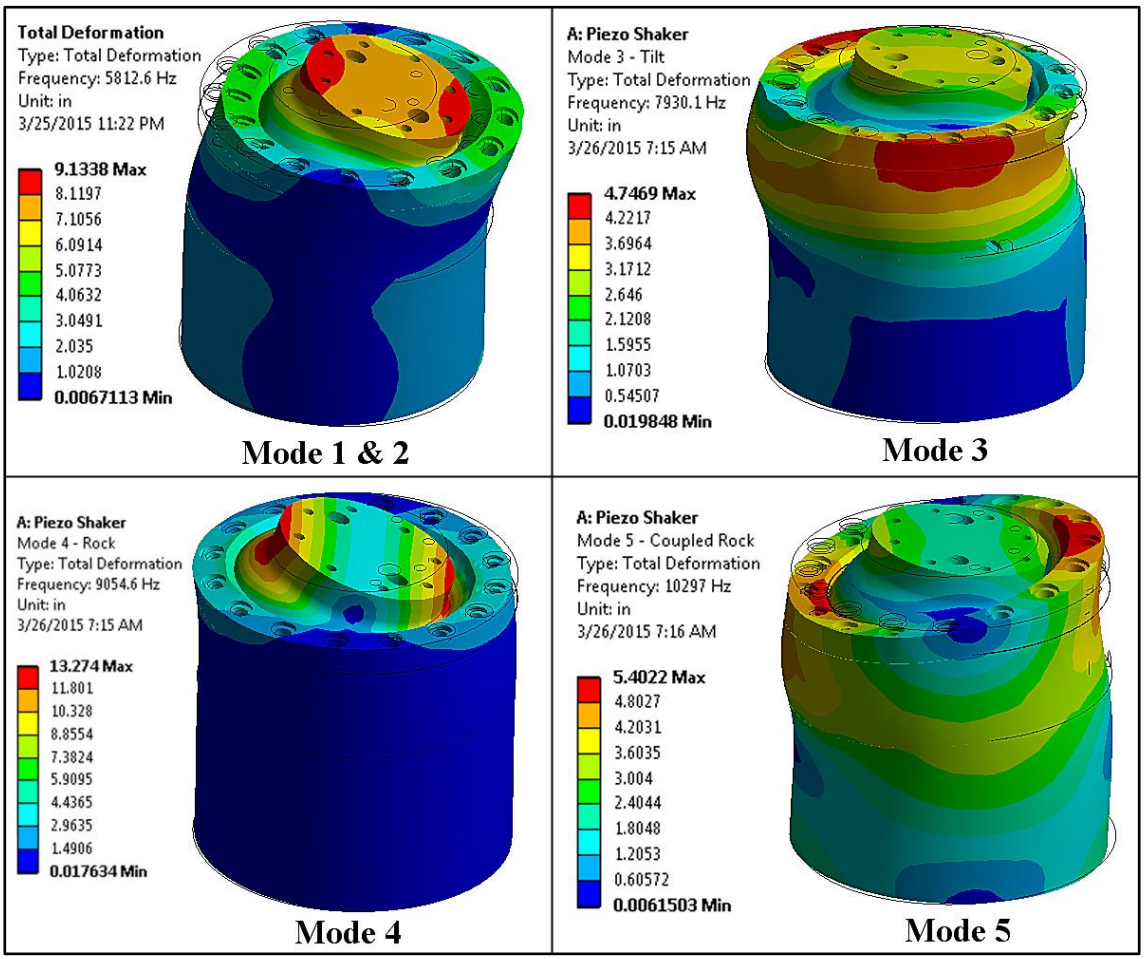

Figure 32. First Five Piezoelectric Shaker Modes

The modes shown in Figure 32 and compared to the ping data in Table 15 are ones produced by the FEM with shapes that would be captured using single point laser vibrometer test setup described in Chapter III. The FEM predicted six other modes, shown in Figure 33. These modes where in the 0 Hz to 10,000 Hz frequency range of the first five modes, however, the modes where not detected by the ping test because their shape produced no displacement at the laser measurement point, as is the case for all six modes shown in Figure 33, or because the energy introduced into the system by the ping hammer was not sufficient to excite the mode.

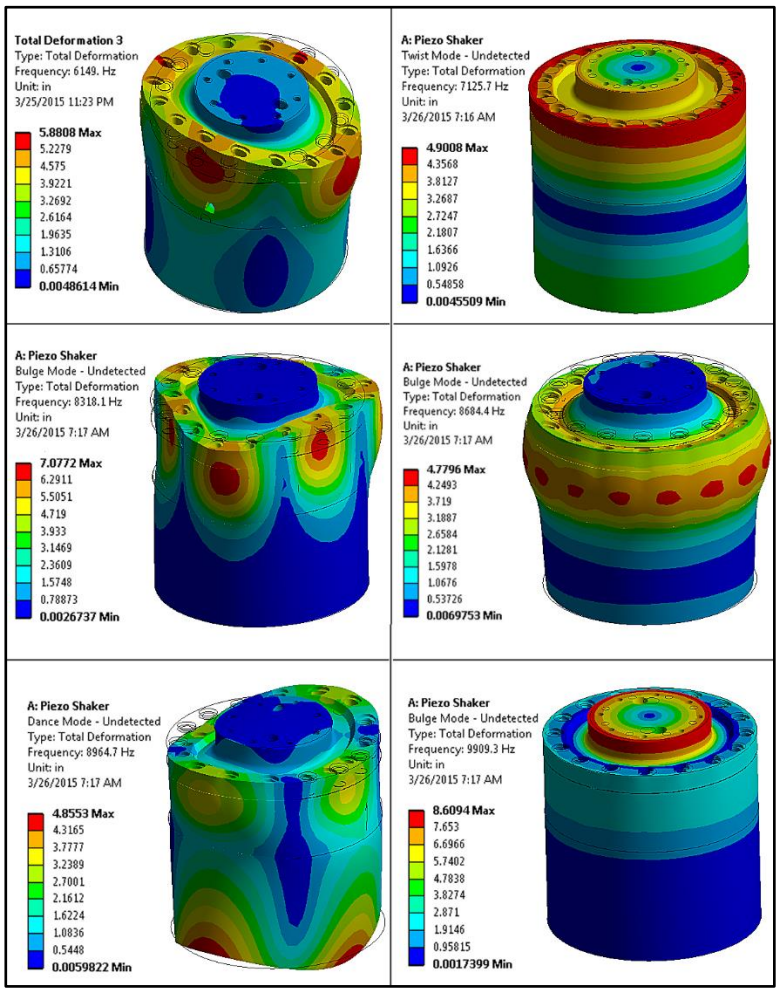

Figure 33. Ping Test Undetected Mode Shapes

The piezoelectric shaker has empty areas inside when assembled that fully contains air. To ensure that the boundaries in contact with free space were correctly modeled as free surfaces the values for normal and shear stress were evaluated in the free boundaries to check if they were zero, as required of material mechanics. To accomplish this check, a real force had to be introduce to the system through a harmonic analysis, and a 500lb sinusoidal forcing function was applied to the bottom of the lid surface as described in the methodology. The force was applied because finite element model does not include the piezoelectric constitutive relationships for the electrical response, therefore to produce a true mechanical response, a sinusoidal force equivalent to the applied 42 V input was calculated using the simplified model force calculation of Equation (21). This force was used to produce the harmonic excitation in the finite element model harmonic analysis.

A representation of the normal and shear stress for the first mode is shown in Figure 34. The normal and shear values reported by ANSYS were not exactly zero, but they were very near zero when compared to the overall 500 psi to 1,000 psi stress in the system. An additional simulation was run using an ANSYS HSFLD242 contained fluid element to represent the contained air, and normal and shear stress changes were found to be negligible. Therefore, it was concluded air is not required in the finite element model.

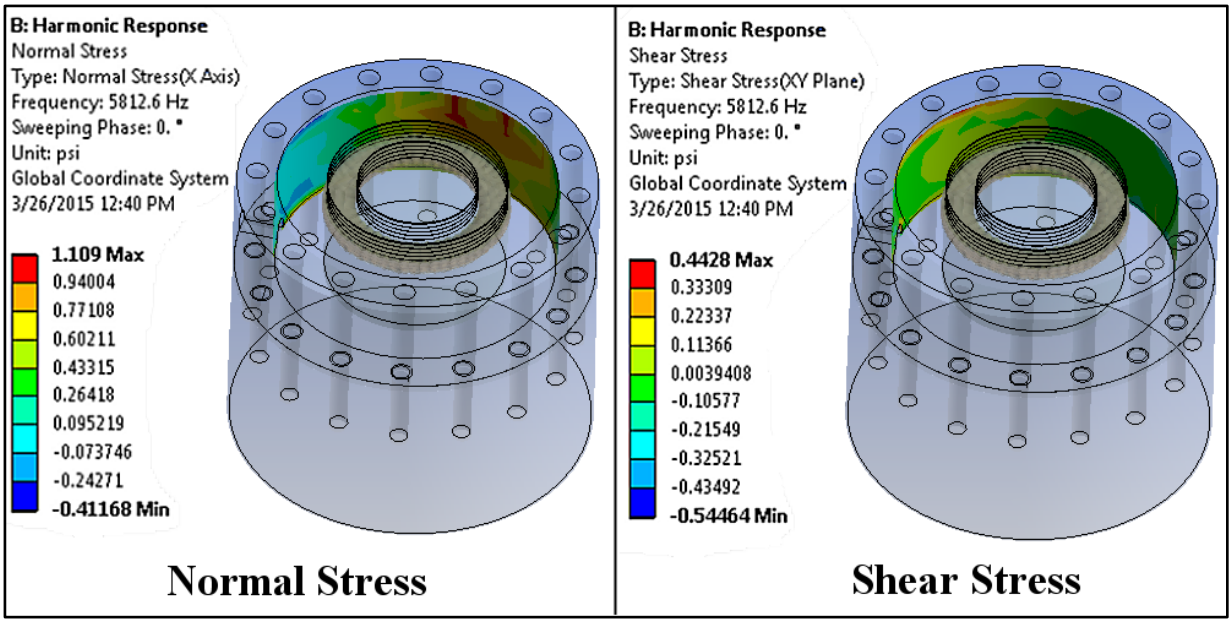

Figure 34. Free Surface Normal and Shear Stress

A final set of results was produced by comparing the shaker table response, obtained when operating the table at 30 mV input voltage, to the ping data. The comparison of the piezoelectric table physical response and experimental ping data is shown in Figure 35. The results shown in Figure 35 were produced by normalizing the velocity amplitude of the test data by the largest amplitude value so the natural frequencies could be compared. This was necessary because the velocities produced by operating the table at 42 V were much higher than those introduced to the system with a small ping hammer.

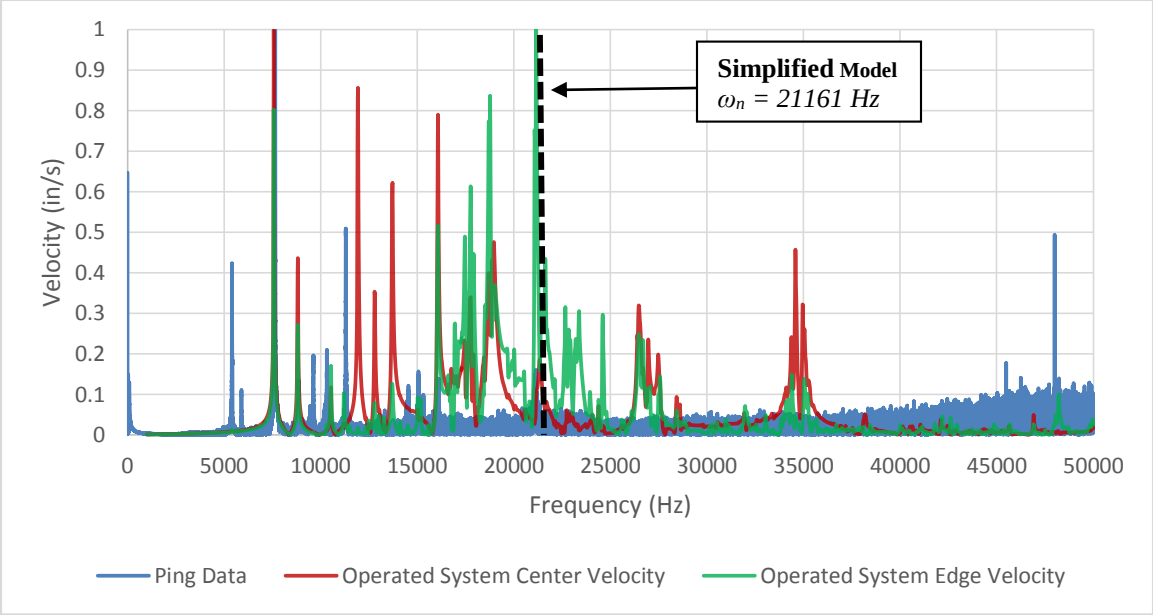

Figure 35. Ping and Physical System Response Comparison

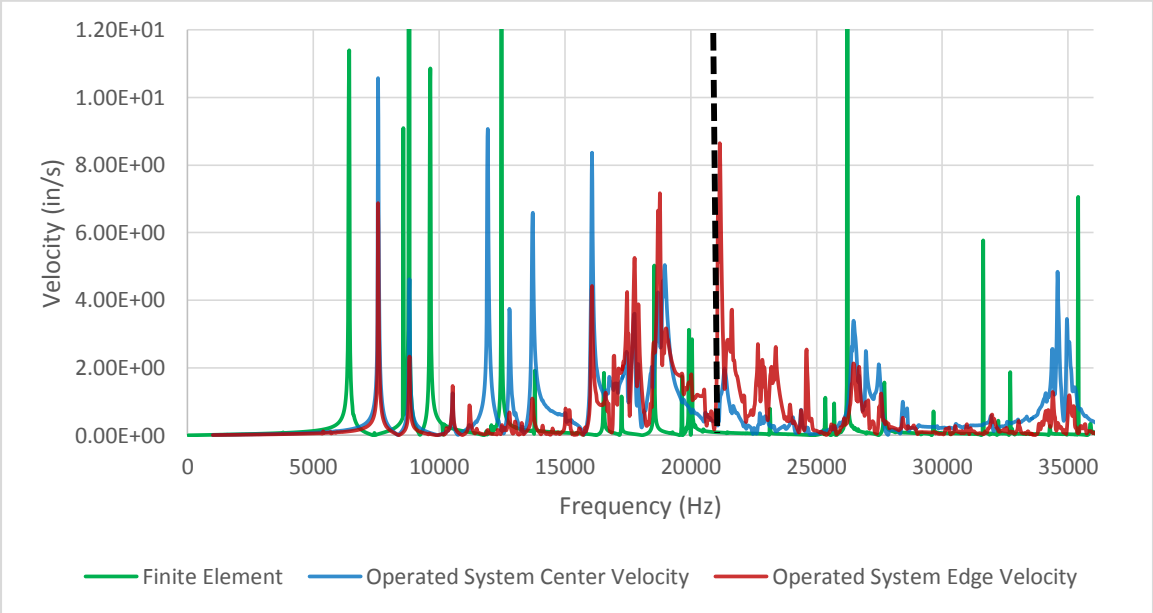

Figure 36. Finite Element and Physical System Response Comparison

According to vibration theory, applying a harmonic forcing function to the piezoelectric shaker table should not affect the natural frequencies of the system because the natural frequency values are calculated for the homogeneous portion of the differential equation of motion where the forcing function is taken as zero. However, the results of Figure 35 indicate that the natural frequencies of the free response and the forced response natural frequencies do not coincide. This result was expected because the excitation that was applied to the shaker table was generated internally by the piezoelectric crystals. The crystals have a mechanical response which is coupled to the electrical excitation and this effect was not investigated as part of this thesis work, but was left as an extension for future work. Therefore, as the crystals are excited, their stiffness changes according to the piezo material elasticity constants matrix and the natural frequency of the system can be affected as indicated in Figure 35.

Figure 36 also represents a comparison between a physical system response which includes the electromechanical coupling and a finite element model that does not. This was a known limitation of the finite element model when beginning this thesis work since only the mechanical properties of the shaker were entered into the analysis. In addition, the forcing function used to produce the results of Figure 36 was derived from the simplified 1D model of the shaker and also introduced some error to the analysis. Despite these limitations, the finite element model did predict most of the modes within 15% of their actual values and the simplified SDOF model predicted a natural frequency within 2% of a mode.

However, there were natural frequencies in the physical system response data which the finite element model did not predict. These modes were between the 21000 Hz to 25000 Hz range, and were captured by edge laser measurements when the center laser indicated little motion, as shown in Figure 36. Measurements where the edge of the shaker table test area displaces while the center remains nearly stationary, indicates rocking mode shapes similar to the one shown in Figure 37. Mode shapes like this would not be indicated in the finite element model frequency response plot because it was created by averaging the displacement and velocity of the shaker table test area surface. With this type of mode shape, the average velocity and displacement values would be zero because of the symmetry of the mode. This is likely the reason the finite element model did not predict these natural frequencies.

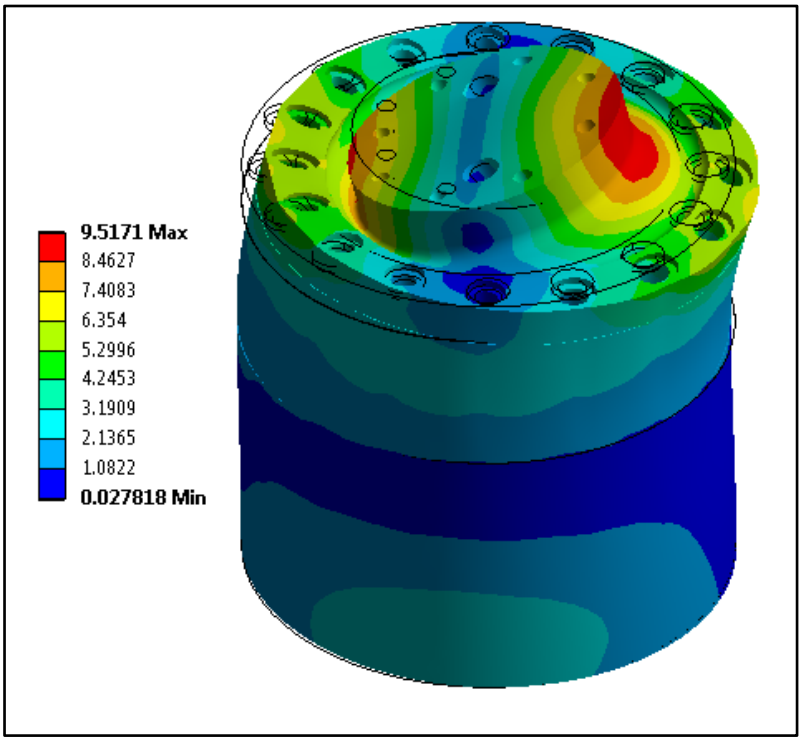

Figure 37. Finite Element Rocking Mode Shape

Unfortunately, mode shapes where the edges displace but the center does not, like the one shown in Figure 37, are shapes that would produce large moments in the piezoelectric crystals and are likely to cause them to break. Therefore, predicting these natural frequencies is an important aspect of analyzing the piezoelectric shaker table. The easiest way to accomplish this in the finite element simulation is to add an additional frequency response plot based on the maximum velocity and displacement value of lid test area rather than the average value. A plot of this response data is shown in Figure 38, and it indicates the natural frequencies in the range of the missing modes are predicted. Overall, producing both the average and maximum test area displacement and velocity frequency response plots and using them in combination is the best approach to predict the modal characteristics of the piezoelectric shaker table.

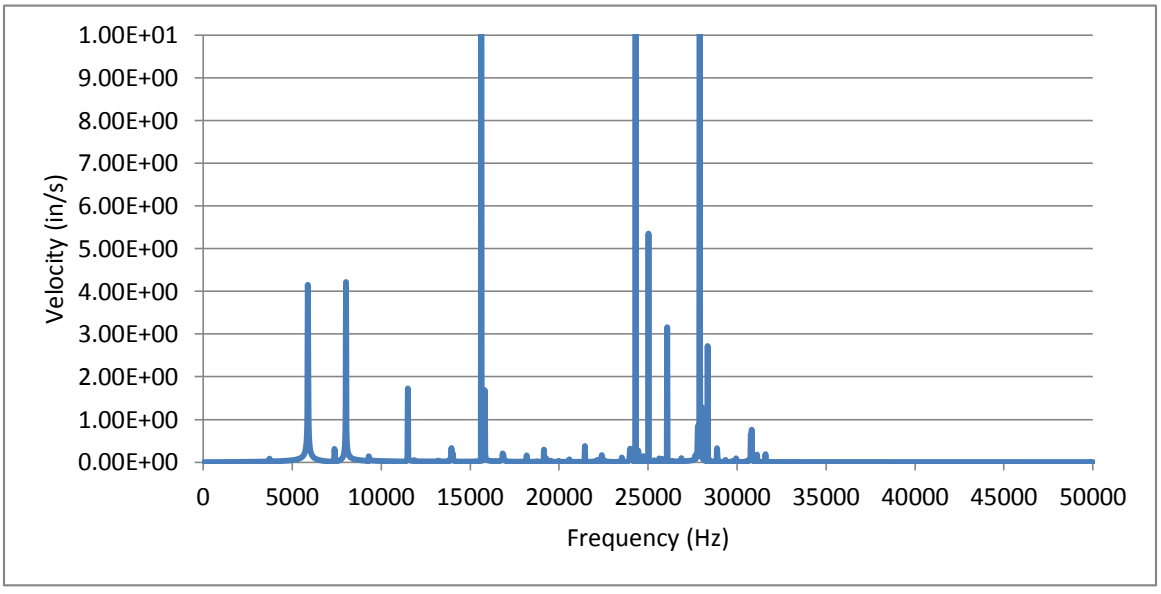

Figure 38. Finite Element Response Using Maximum Surface Velocity

Summary

Several preliminary results were produced and used to obtain the final system finite element results. These final results were compared to ping test data and previously collected data for the physical system response. The finite element model was found to match the first natural frequency of ping data within 10% and predict most natural modes for the operated piezoelectric table. However, the finite element model only accounted for mechanical response and did not include electromechanical coupling, so the predicted modes for the operational table were not able to be predicted. This was a known limitation of this preliminary research and adding the coupling effects of the piezoelectric materials was left for future research. Overall, the results indicate that the model can be useful in its current state when multiple frequency response plots are used in combination to predict natural frequencies of the operational table.

V. Conclusions and Recommendations

Chapter Overview

The purpose of conducting research is to obtain results and draw conclusions. Conclusions are discovered by carefully considering the results of the research to determine new facts and principles. When considering the results it is common for a researcher to also find areas which they feel can be improved. These areas of improvement are often vocalized as recommended actions for future researchers.

This chapter follows the outline above by first explaining the conclusions that were determined based on analysis and results obtained from the piezoelectric shaker table. These conclusions were used to produce recommended actions and suggestions for recommended future research. All of the piezoelectric shaker research conclusions and recommendations were then summarized in several lists that can be quickly referenced.

Conclusions of Research

The research topic of this thesis work required multiple steps, and it generated numerous results. The steps included both experimentation and analysis to obtain data and produce the results. Multiple conclusions were drawn from these steps throughout the process of completing this thesis. The most significant of these conclusions is emphasized and explained in this section.

The simplified model that was created as an initial investigation into the piezoelectric shaker table yielded several important conclusions. First, the magnitude of the beam and piezoelectric stack stiffness indicated the beam or lid fillet, has a negligible effect on the natural frequency of the system. The beam calculation shown in this thesis

work assumed a rectangular cross section, but even when the moment of inertia was updated to account for the disk shape of the fillet, the beam still had little effect on the natural frequency. This conclusion indicates any calculation for the simplified model could ignore the beam stiffness terms because they had negligible impact on the solution.

Next, the natural frequency prediction of the simplified model was very close to modes of both the experimental ping data, and the operational system response data. It was also very close to the range in which the mode shapes could produce significant bending moments in the piezoelectric crystals. Through these results, it was concluded the simplified model is an excellent tool for quickly determining critical natural frequencies to avoid. The equations developed to characterize this model also resulted in several supplemental relationships, which could be used to determine other important values, and these equations were also considered to be excellent tools for planning and early calculations.

The FABCEL material used in the study of material properties for this thesis was designed as an isolation pad, but during the course of this work, under specific conditions, its properties were found to approximate a free-free boundary condition. The FABCEL 25 neoprene pad produces free-free boundary conditions when the test item natural frequencies are well above the natural frequency of the pad itself. Although it is recommended additional research be conducted on the FABCEL material, it was concluded using at least a 10:1 ratio for the test item natural frequency to support natural frequency provides sufficient isolation efficiency to approximate free-free condition in most cases.

As mentioned previously, the isolation pad was used to help determine material properties of the base, collar, lid, and spacer shaker table components. These properties were tuned in the component finite element models until the first natural frequency of the FEM agreed with the experimental ping data. Through this process, it was discovered the actual material properties of components vary significantly from typical published values. This result was expected since it was known variations in manufacturing can produce different properties, but the material tuning results still emphasized the need to analyze material properties when conducting FEA which are sensitive to small variations in these properties.

During this research, the effects of electromechanical coupling were highlighted when system ping test data was compared to operational system response data. Ignoring the polarization of the piezoelectric crystals, the ping test natural frequencies were expected to coincide with those of the operated system because applying a harmonic forcing function should not alter these characteristics. However, during the system response tests, the test table was excited by operating the crystals, and it was observed the modes of the operated table and ping tests did not agree. This observation led to the conclusion the natural frequency of the system is affected by the electromechanical coupling properties of the piezo crystals. Additionally, during the operational tests, the applied system input voltages were varied from 5 mV to 30 mV for each test, and it was observed this variation caused the amplitude of the frequency response to change, while the natural frequencies remained the same. It was concluded in this typical operating range, input voltage variation has no effect on the natural frequency of the system.

Multiple finite element simulations were also run during the course of this thesis work. Some of these simulations were used to tune the material properties of the shaker table components. This tuning process used measured properties of density, assumed a value of Poisson's ratio from published data, and optimized Young's modulus. Poisson's ratio was fixed because it had lower range variation in published data than Young's modulus, but to insure its effects were not large on the FEA modal analysis it was also investigated. Several additional finite element simulations not directly needed for this thesis work were run to confirm that Poisson's ration had minimal effect on predicted mode shapes, and it was concluded from these simulations changes in Poisson's ratio were negligible for FEA modal analyses.

The most pertinent conclusion drawn from the results of this research was a range of frequencies to avoid when operating the piezoelectric shaker table. These modes were discovered using a two laser vibrometer measuring technique, which captured physical response of the operated table at the center and edge of the test area. The lasers recorded mode shapes in which the center of the test area remained nearly stationary, while the edges of the test area experienced displacement. These modes had potential to produce bending moments which are destructive for piezoelectric crystals at low levels. The captured modes occurred in a range known to have caused problems for the TEFF in the past, and these modes were also predicted by the FEM when maximum displacement of the test area was observed in a harmonic analysis. Overall, the test data and FEM support the conclusion that the frequency range of 21,000 Hz to 25,000 Hz should be avoided when operating the AFRL piezoelectric shaker table.

Recommendations for Action

Although the model developed as part of this thesis work is not yet complete, it can still be used to approximate the modes of the system and run simulated fatigue tests with complex fixture designs. Approximating natural frequencies using the system FEM should give the TEFF a general range of frequencies to avoid in order to prevent shattering costly crystals. In addition, incorporating solid models of turbine engine test components with the existing model and running finite element simulations should allow the TEFF researchers to roughly estimate fatigue and vibrational characteristics of test items. However, these simulations should only be used as a supplement to physical testing at this point since the model is not complete and results are not exact. If the model is used with the understanding that limitations currently exist, it can still be of use until the electrical properties of the piezoelectric crystals can be implemented to increase the fidelity of the analysis.

Overall, it is recommended that the TEFF begin using the models produced in this thesis for fatigue test development. Obtaining preliminary results by running a finite element simulation can be a quick check that provides rough estimates for crafting a test plan. The accuracy of the current model is sufficient and well suited for early predictions that would be required during the planning phase of an experiment.

Recommendations for Future Research

This thesis work was completed as an initial step in the overall goal of producing a piezoelectric shaker table finite element model which accounts for both the electrical and mechanical properties of piezo crystals. The current model was designed only to

account for the mechanical properties and the electrical characteristics were not implemented in the FEA. The first step in future work on this topic should be to fully characterize the piezoelectric crystals and implement their electrical properties into the finite element model. In addition, the current work assumed published values for crystal Poisson's ratio and Young's modulus because the method used in testing these values for other components was not adequate for the crystals. However, as work progressed it was discovered that there is 25% difference in the range of published values for this material. If tests will be conducted to characterize the electrical properties, a subset of tests should be added to confirm these two mechanical properties of the crystals. The test method used in this thesis was also not adequate to characterize the copper electrode material properties and they should also be confirmed even though a smaller range of published values exists.

The FABCEL isolation pad used for material ping testing also requires further investigation. Additional ping tests should be performed with varying stiffness materials to better characterize the threshold at which this material can be said to approximate free-free boundary conditions. In this thesis work, the natural frequency ratios of the FABCEL support and shaker table components were very large, with the exception of the crystals and electrodes, and there was no question that free-free conditions were approximated. The loads associated with the components also fell in a linear region of the FABCEL materials load-deflection curve, further simplifying the calculation. The frequency ratios and loads of future items tested are not likely to be exactly the same as those experienced in this work and full understanding of the non-linear load-deflection behavior and threshold frequency ratio will be invaluable for future work.

The system finite element model created as part of this thesis work is fairly complex and requires a significant amount of computing power to run. The current model, which does not include computation of electrical response, is barely able to run on a standard desktop or laptop with 4GB of memory and an accelerated Graphics Processing Unit (GPU). Adding additional fidelity to this model by updating the piezoelectric crystals to include electrical response behavior will require additional computational power that will likely not be available on a standard computer. As future research is conducted, it will be necessary to obtain access to a High Performance Computing (HPC) environment suitable for complex finite element analysis in order to run ANSYS simulations for this model.

System Response testing with the current experimental setup allowed a comparison of natural frequencies (eigenvalues), but not mode shapes (eigenvectors). As complexity of the model increases, an experimental setup which can characterize the mode shapes should be considered so that modal comparisons can be based on both frequency and shape. The TEFF owns a laser scanning vibrometer which has the capability to produce 2D results and it is recommended that future modal characterization research use this equipment to obtain response data.

Summary

The data and results obtained for the piezoelectric shaker table allowed several conclusions and recommendations to be developed. The specific conclusions are summarized below for reference:

(1) Simplified mechanical model is a good tool for quickly predicting a critical frequency to avoid

(2) Equivalent beam stiffness of the lid fillet is negligible in simplified mechanical model frequency calculations
(3) Simplified mechanical model supplemental equations are useful tools in predicting system displacement amplitude, applied force, and maximum voltage
(4) FABCEL 25 neoprene isolation pad is provides a good approximation of free-free conditions for frequency ratios of 10:1 or better
(5) The frequency range of 21000 Hz to 25000 Hz can produce bending moments which shatters crystals and should be avoided in testing
(6) Material properties should be determined experimentally for research dependent on and sensitive to these properties
(7) Operating voltages in the range of 5 mV to 30 mV have no effect on the natural frequency of the operational piezoelectric system
(8) Operating the piezoelectric crystals couples the electromechanical response and affects the natural frequency of the system
(9) Variation in Poisson's ratio has negligible effects on the system FEM

The specific recommendations for future research are also summarized below for reference:

(1) Experimental testing to characterize electrical properties of piezoelectric material
(2) Experimental testing to characterize mechanical properties of piezoelectric material and copper electrode
(3) Study of FABCEL 25 isolation pad non-linear behavior and threshold frequency ratio to for free-free boundary condition approximation
(4) Obtain access to HPC environment with ANSYS installed
(5) Conduct system response testing with a laser scanning vibromerer to measure mode shapes in addition to natural frequencies

Only a single recommendation for action was determined from this work. This recommendation is that the TEFF should integrate the model, in its current state, only as a tool in test planning and should continue work towards completing the model by implementing the electrical properties of the piezoelectric crystals.

Overall, the work completed during the course of this thesis was an important initial step in creating a finite element model that can accurately characterize the modal parameters of a piezoelectric shaker table. The current work only incorporates the mechanical response of the piezo crystals, but its simulation predictions are within 10-15% of actual modes and it should still be a valuable tool, at certain frequencies, which can benefit the Air Force Research Laboratories.

Appendix

Appendix A: Piezoelectric Shaker Table Component Dimensions

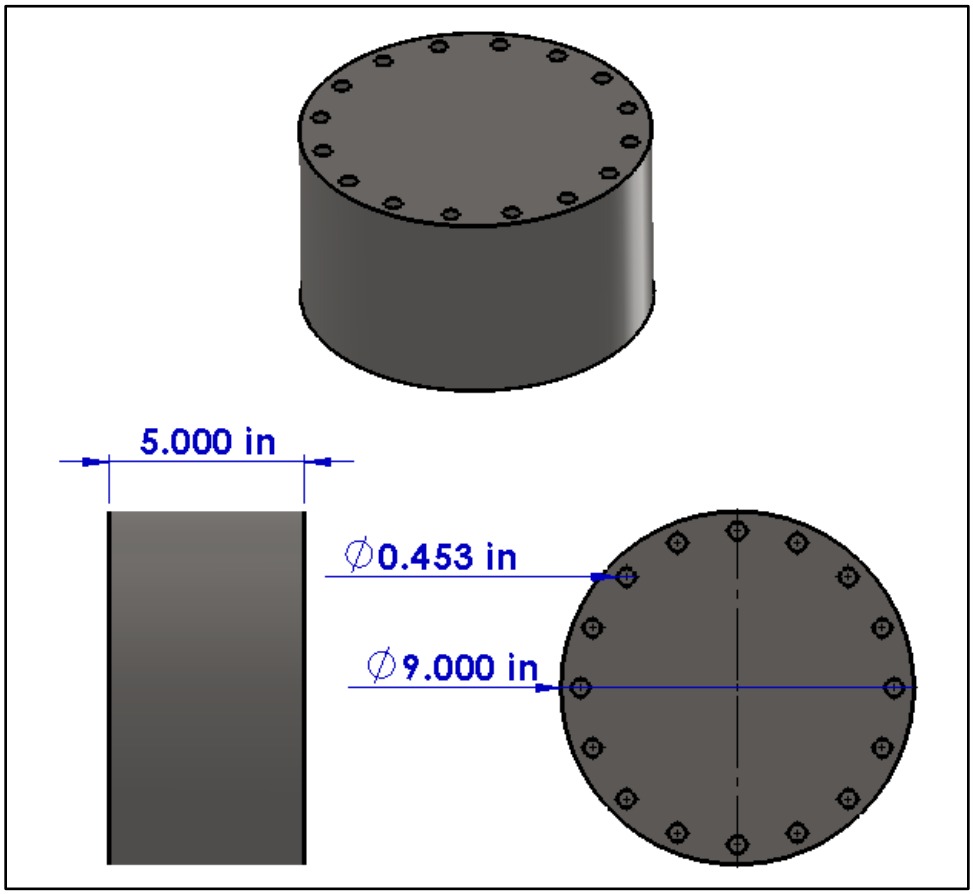

Figure 39. Piezoelectric Shaker Table Base Component Dimensions

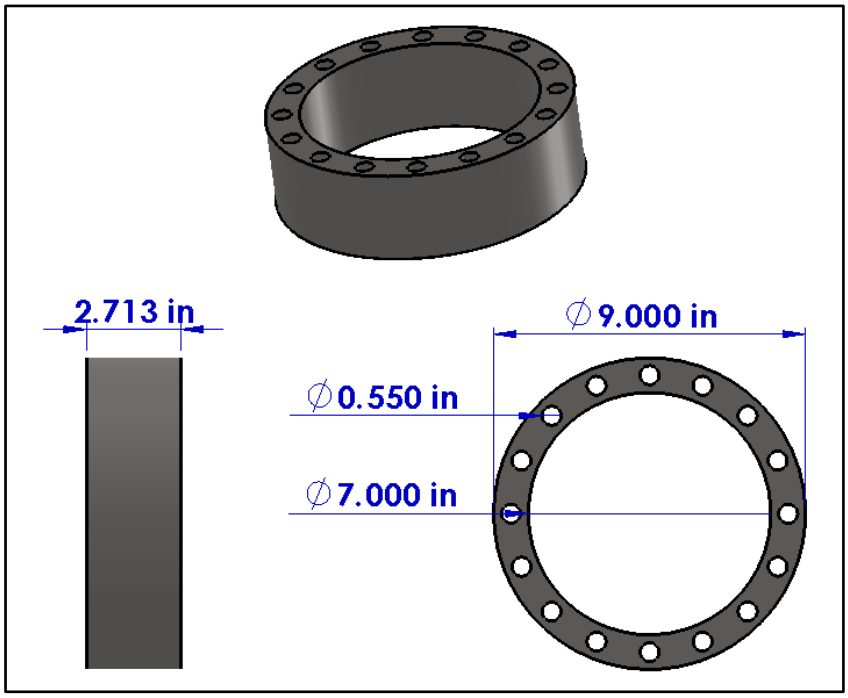

Figure 40. Piezoelectric Shaker Table Collar Component Dimensions

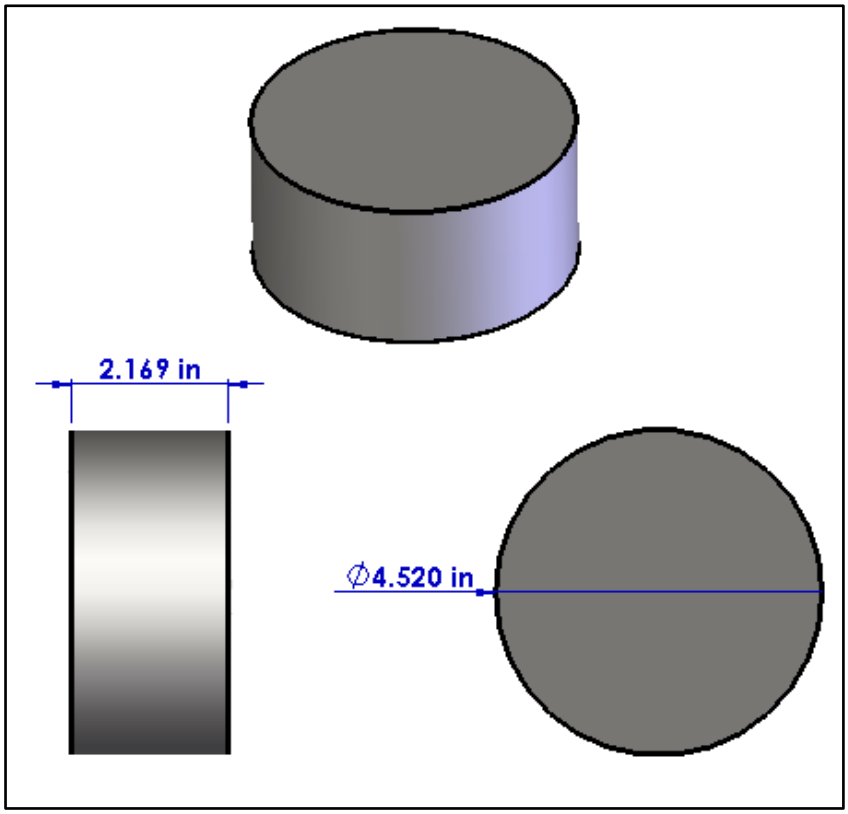

Figure 41. Piezoelectric Shaker Table Spacer Component Dimensions

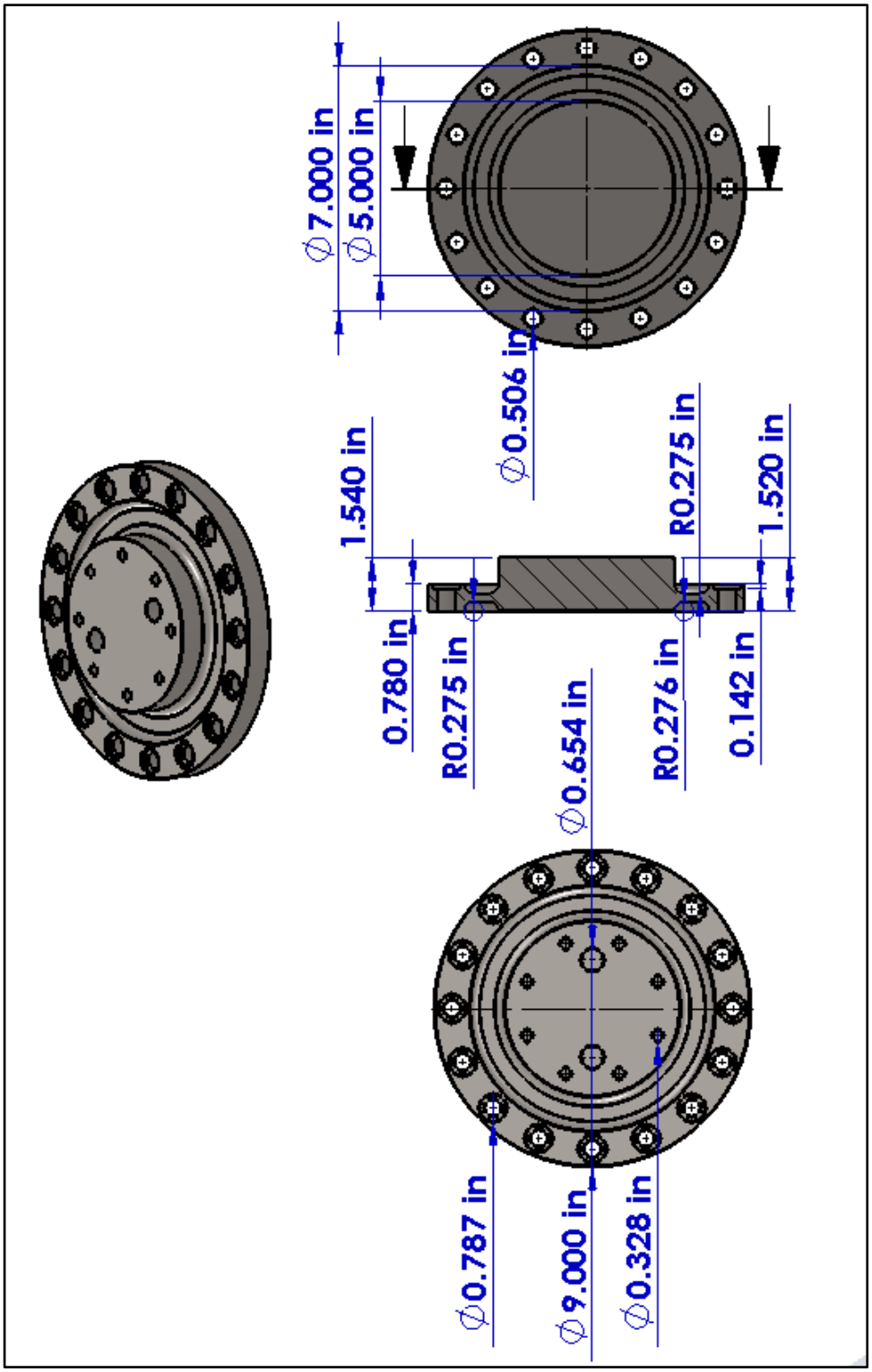

Figure 42. Piezoelectric Shaker Table Lid Component Dimensions

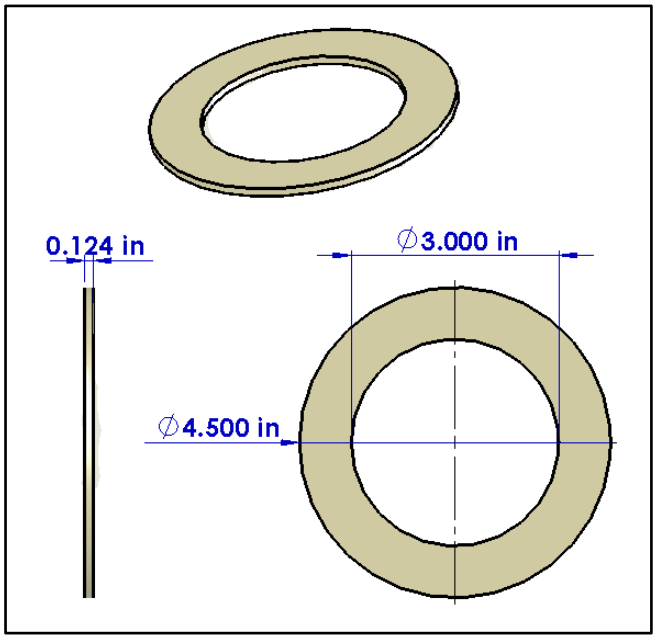

Figure 43. Piezoelectric Shaker Table Crystal Component Dimensions

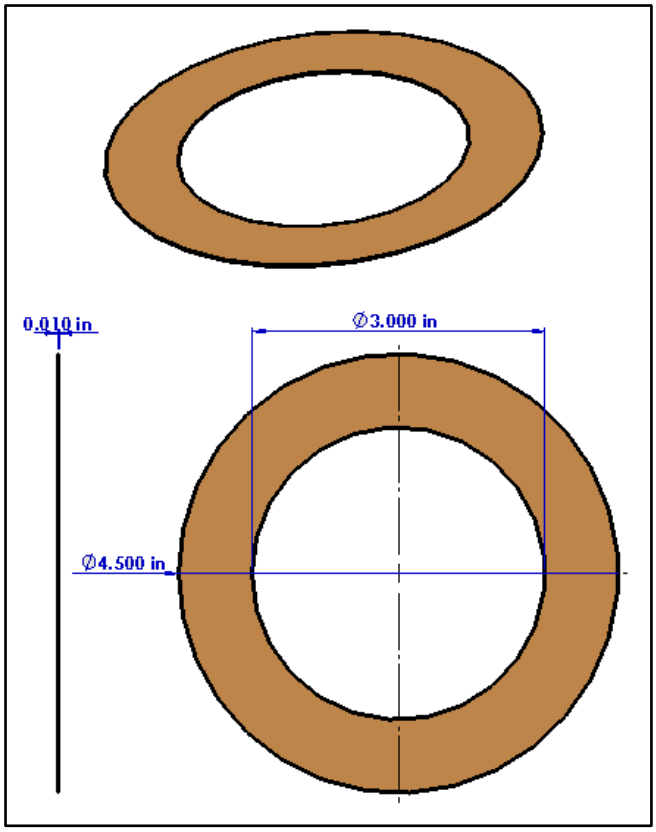

Figure 44. Piezoelectric Shaker Table Electrode Component Dimensions

Appendix B: Extracted FABCEL 25 Data Sheet Information

Table 16. Extracted FABCEL Load-Deflection Data

Deflection (in)	Load (psi)
0.00E+00	0.0853
1.73E-03	0.5985
5.19E-03	1.4535
8.65E-03	2.4796
1.21E-02	3.3346
1.56E-02	4.3606
1.90E-02	5.3866
2.25E-02	7.0964
2.59E-02	8.2934
2.94E-02	10.0031
3.29E-02	12.3967
3.63E-02	14.7902
3.98E-02	17.5255
4.32E-02	20.7738
4.67E-02	23.6802

References

ANSYS Documentation. ANSYS Help Viewer. Canonsburg, PA: ANSYS Inc., 2014.

Bhat, S. and Patibandla, R. "Metal Fatigue and Basic Theoretical Models: A Review," in *Alloy Steel – Properties and Use*. Ed. Dr. Eduardo Velencia Morales. Intech, 2011.

Campbell, G. S. "A Note on Fatal Aircraft Accidents Involving Metal Fatigue," *International Journal of Fatigue*, 3: 181-185 (October 1981).

Carne, T. G. and others. "Support Conditions for Experimental Modal Analysis," *Sound and Vibration*, 7-6 (June 2007).

Cook, D. C. and others. *Concepts and Applications of Finite Element Analysis*. NJ: John Wiley and Sons Inc., 2002.

D'Antonio, P. *Predicting Isolation Efficiency Using Mobilities*. RPG Diffusor Systems, Inc. Upper Marlboro MD, 2010.

"Efunda: The Ultimate Online Reference for Engineers." (n.d.) http://www.efunda.com/home.cfm

FABCEL Pads. FABCEL Product Catalog. Stoughton: Fabreeka International Inc., 1994.

Jordan, T. L. and Ounaies, Z. *Piezoelectric Ceramics Characterization*. Contract NASI-97046. Hampton VA: Langley Research Center, September 2001 (NASA/CR-2001-211225)

Lang, G. F. and Snyder, D. "Understanding the Physics of Electrodynamic Shaker Performance," *Sound & Vibration*, 1-10 (October 2001).

Meirovitch, L., *Fundamentals of Vibration*. IL: Waveland Press Inc., 2010

Meirovitch, L. and Ghosh, D. "Control of Flutter in Bridges," *Journal of Engineering Mechanics,* 113 458-472 (1987)

Moheimani, S. O. and Fleming, A. *Piezoelectric Transducers for Vibration Control and Damping*. London: Springer-Verlag, 2006.

Scott-Emuakpor, O. E. and others. "Development of Gigacycle Bending Fatigue Test Method," *55th AIAA/ASME/ASCE/SC Structures, Structural Dynamics, and Materials Conference*, January 2012.

Pickelmann, L. “First Steps Towards Piezoaction,” *Piezomechanik Katalog*, 7-75 (April 2010)

Payne, B. and others. “Piezoelectric Shaker Development for High Frequency Calibration of Accelerometers,” *The 9th International Conference on Vibration Measurements by Laser and Noncontact Techniques*. 373-382. Maryland: National Institute of Standards and Technology, 2010.

Piefort, V. and Preumont, A. *Finite Element Modeling of Piezoelectric Structures*. Brussels Belgium: Active Structure Laboratory, (n.d.)

Polytec Inc. “Basic Principles of Vibrometry.” (n.d.) http://www.polytec.com/us/solutions/vibration-measurement/basic-principles-of-vibrometry/

Rhoades, C. W. *Characterization of the Accuracy in A Reverse Engineering Process Employing White Light Scanned Data to Develop Constraint-Based Three Dimensional Computer Models*. MS Thesis. Western Carolina University, Cullowhee NC, 2011.

Ricci, S. and others. “Virtual Shaker Testing for Predicting and Improving Vibration Test Performance,” *IMAC-XXVII: Conference & Exposition on Structural Dynamics – Model Verification and Validation*. 1-5. Orlando FL: Università di Bologna, 2009.

Rieger, N. F. *The Relationship Between Finite Element Analysis and Modal Analysis*. Stress Technology Inc. Rochester NY, (n.d.)

Schūtz, W. “A History of Fatigue,” *Engineering Fracture Mechanics*, 2: 263-300 (1996).\

Shu-Hong, X. and others. “Virtual Vibration Test and Verification for the Satellite”. *14th International Congress on Sound and Vibration.* 1-7. Cairns Australia: Beijing Institute of Spacecraft Environment Engineering, 2007.

Uyema, M. and others. “Finite Element Method for Active Vibration Suppression of Smart Composite Structures using Piezoelectric Materials,” *Journal of Thermoplastic Composite Materials*, SAGE Publications, 19(3), 309-352 (2006).

REPORT DOCUMENTATION PAGE

Form Approved
OMB No. 074-0188

1. REPORT DATE *(DD-MM-YYYY)*	**2. REPORT TYPE**	**3. DATES COVERED** *(From – To)*
18-06-2015	Master's Thesis	March 2014 – June 2015

TITLE AND SUBTITLE

Modal Characterization of a Piezoelectric Shaker Table

5a. CONTRACT NUMBER

5b. GRANT NUMBER

5c. PROGRAM ELEMENT NUMBER

6. AUTHOR(S)

Hodkin, Randall J., Captain, USAF

5d. PROJECT NUMBER

5e. TASK NUMBER

5f. WORK UNIT NUMBER

7. PERFORMING ORGANIZATION NAMES(S) AND ADDRESS(S)
Air Force Institute of Technology
Graduate School of Engineering and Management (AFIT/ENY)
2950 Hobson Way, Building 640
WPAFB OH 45433-8865

8. PERFORMING ORGANIZATION REPORT NUMBER

AFIT-ENY-MS-15-J-001

9. SPONSORING/MONITORING AGENCY NAME(S) AND ADDRESS(ES)
Turbine Engine Fatigue Facility
1950 5th St B20018D RD136
(937) 255-7299
(Tommy.George@us.af.mil)
ATTN: Dr. Tommy George

10. SPONSOR/MONITOR'S ACRONYM(S)

AFRL/RQTI

11. SPONSOR/MONITOR'S REPORT NUMBER(S)

12. DISTRIBUTION/AVAILABILITY STATEMENT
DISTRUBTION STATEMENT A. APPROVED FOR PUBLIC RELEASE; DISTRIBUTION UNLIMITED.

13. SUPPLEMENTARY NOTES
This material is declared a work of the U.S. Government and is not subject to copyright protection in the United States.

14. ABSTRACT

Piezoelectric actuated shaker tables are often used for high frequency fatigue testing. Since natural frequencies can appear in the operating range of these shaker tables, it is necessary to conduct modal characterization of the system before testing. This thesis describes the design and experimental validation of a mechanical model used for modal analysis of a piezoelectric shaker table. A commercially available three-dimensional scanning device was used to produce a point cloud model of the surface geometry, which was converted to a solid model and imported into a Finite Element Analysis (FEA) package for modal analysis. Using a laser vibrometer to measure displacement and velocity, the physical vibration response of the shaker table was obtained for comparison with FEA frequency response results. The laser vibrometer data was used to validate and tune the FEA modal response.

15. SUBJECT TERMS
Piezoelectric, Shaker Table, Vibration, Fatigue, Modal Analysis, Finite Element, Solid Model, CAD

16. SECURITY CLASSIFICATION OF:			**17. LIMITATION OF ABSTRACT**	**18. NUMBER OF PAGES**	**19a. NAME OF RESPONSIBLE PERSON**
a. REPORT	**b. ABSTRACT**	**c. THIS PAGE**			Dr. Anthony Palazotto, AFIT/ENY
U	**U**	**U**	**UU**	112	**19b. TELEPHONE NUMBER** *(Include area code)* (937) 255-6565, ext 4599 (Anthony.Palazotto@afit.edu)

Standard Form 298 (Rev. 8-98)
Prescribed by ANSI Std. Z39-18